Enhancement of Heat Transfer in Two Pass Solar Air Heater Duct Using Multi V-Shaped Rib Geometry

Dissertation

Submitted in partial fulfilment of the requirements

for the degree of

MASTER OF TECHNOLOGY

In

THERMAL ENGINEERING

By

RAVI KANT

(2K13/THE/18)

Under the guidance of

Mr. Raghavendra Gautam

Asst. Prof. Department of Mechanical Engineering

Delhi Technological University

Delhi, India

Department of Mechanical Engineering

Delhi Technological University

(Formerly Delhi College of Engineering)

Delhi

July 2016

DELHI TECHNOLOGICAL UNIVERSITY

Established by Govt. of Delhi vide Act 6 of 2009

(*Formerly Delhi College of Engineering*)

Shahbad Daulatpur, Main Bawana Road, Delhi-110042

CERTIFICATE

This is to certify that this dissertation, entitled **ENHANCEMENT OF HEAT TRANSFER IN TWO PASS SOLAR AIR HEATER DUCT USING MULTI V-SHAPED RIB GEOMETRY**, is the authentic work carried out by **Mr. Ravi Kant (2K13/THE/18)** under my guidance and supervision in partial fulfilment for award of degree of **Master of Technology (M. Tech)** in **Thermal Engineering** by Department of Mechanical Engineering in Delhi Technological University (Formerly Delhi College of Engineering), Delhi during the year 2013-2016.

As per the candidate declaration, this work has not been submitted elsewhere for the award of any other degree.

(Signature of Guide)	*(Signature of HOD)*
Mr. Raghavendra Gautam	Dr. R.S Mishra (HOD)
Asst. Prof. Department of Mechanical Engg	Department of Mechanical Engg
Delhi Technological University	Delhi Technological University

DECLARATION

I, hereby, declare that the work being presented in this dissertation, entitled **ENHANCEMENT OF HEAT TRANSFER IN TWO PASS SOLAR AIR HEATER DUCT USING MULTI V-SHAPED RIB GEOMETRY**, is an authentic record of my own work carried out under the guidance of **Mr. Raghavendra Gautam**, Asst. Prof. Mechanical Engineering Department, Delhi Technological University (Formerly Delhi College of Engineering), Delhi. The work contained in this dissertation has not been submitted in part or full, to any other university or institution for award of any degree or diploma.

This dissertation is submitted to **Delhi Technological University** (Formerly Delhi College of Engineering) in partial fulfilment for the **Master of Technology (M. Tech)** in **Thermal Engineering** during the academic year 2015-2016.

_____

(Signature and Name of Student)

Ravi Kant

(2K13/THE/18)

ACKNOWLEDGEMENTS

I would like to express my gratitude to my Guide Mr. Raghavendra Gautam for the useful comments, remarks and engagement through the learning process of this master thesis. Also, I like to thank the classmates, who have willingly shared their precious time during the process of thesis. I would like to thank my parents and loved ones, who have supported me throughout entire process, both by keeping me harmonious and helping me putting pieces together. I will be grateful forever for your love.

ABSTRACT

Energy is basic requirement for the development of nation. The consumption of energy is the index of prosperity of nation. So for the sake of development we should focus more and more on renewable energy sources. Solar energy is emerged as one of the best method of renewable energy source in current waking scenario. Therefore on the lines of contemporary energy requirements, this project is conducted to enhance heat transfer by means of using two pass solar air heater. We have used multi v-shaped discrete rib geometry on the back side of gi sheet roughened absorber plate while following ASHRAE standards. Experiment is conducted with keeping roughness pitch and roughness height constant along with angle of attack constant throughout with varying relative gap distance while keeping outlet temperature of smooth plate as a reference. The experimental outcome showed enhanced nusselt number and heat transfer co-efficient as comparison to smooth plate.

TABLE OF CONTENTS

List of Figures

List of Graphs

List of Tables

CHAPTER - 1

INTRODUCTION

1.1 Energy

Energy is basic requirement for the development of nation. The consumption of energy is the index of prosperity of nation. It provides additional economic value by preserving the resource base and reducing pollution. The limited sources of conventional fuels have directed researchers' attention to renewable energies in recent years. Energy is the one of the major input for economic development of any country. In the case of the developing countries, the energy sector assumes a critical importance in view of the ever increasing energy needs requiring huge investments to meet them. Developing country like India having population about 75% of world consumes 25% of energy. The development rate of the nation is measured by the energy consumption rate in various fields like industrial organisation, defence, domestic purposes and agricultural production.

1.2 Types of Energy Sources

There are two types of energy sources as follows-

1. Renewable Energy sources
2. Non-Renewable Energy sources

1.2.1 Renewable energy sources - Renewable energy sources are those which are virtually inexhaustible and can be replenished after their use. They are biomass based source and are available in unlimited amount in nature. These included-

(i) Solar energy

(ii) Wind energy

(iii) Hydro energy

(iv) Geothermal energy

(v) Ocean energy

(vi) Biomass energy

(vii) Nuclear energy (can also be considered as a renewable source, if atomic minerals are used in fast breeder reactor.)

1.2.2 Non-Renewable energy sources - Non-Renewable energy sources are those natural resources which are exhaustible and cannot be replenished once used. These are developed over a long period due to physical, chemical and biological action below the earth surface. They are available in limited amount. These included-

- Fossil Fuels
    a. Coal
    b. Oil and
    c. Natural Gas

1.3 Solar Energy

Solar energy is a very large, inexhaustible source of energy. It is produced and radiated by the sun more specifically, the sun's energy that reaches to the earth. Solar energy which is the primary source of all kind of energy on the earth, originated in the sun as a result of thermonuclear fusion reaction. Sun can be considered as a large sphere containing helium gas, which is continuously producing hydrogen through fusion reaction and liberating a large amount of heat energy. This energy is radiated by the sun in the form of electromagnetic radiation of which 99% having their wavelength in the range of 0.20 to 0.4μm. Solar power reaching at the top of the atmosphere is about 10^{17} watts and that on earth surface is 10^{16} watts, which total power requirement of the world, is 10^{13} watts. Solar energy systems consist of many parts. The most important part of these systems is the solar collector which collect the sun's energy and to convert it into either electrical power or thermal energy.

1.4 Advantages of Solar Energy

(i) Available everywhere on the earth surface

(ii) Superior in quality

(iii) Quantitatively abundant

(iv) Inexhaustible for all practical purposes, and

(v) No polluting effect on the environment when converted in useful form and utilization

1.5 Application of Solar Energy

(i) Direct method - The direct means include thermal and photovoltaic conversion.

(ii) Indirect method- The indirect means include the use of water power, the winds, biomass, and wave energy and the temperature differences in ocean.

(iii) Solar power generation

(iv) Solar distillation and desalination

(v) Solar drying

(vi) Solar space heating

(vii) Solar cooking, and

(viii) Cold storage for food preservation

1.6 Limitations of Solar Energy

(i) Its availability is intermittent i.e. only available during the day

(ii) It is a dilute source of energy

(iii) It also dependent on the climatic and weather conditions

1.7 Solar Constant

The rate at which solar energy arrive at the top of the atmosphere is called the solar constant (I_{sc}). This is the amount of energy received in unit time on a unit area perpendicular to the sun's direction at the mean distance of the earth from the sun. Since the sun distance and activity vary throughout the year, the rate of arrival of solar radiation also varies. Thus, the so called solar constant is an average from which the actual value varies up to about ±3%. The currently accepted value of solar constant is 1370 W/m^2.

1.8 Heat Transfer and Fluid flow Terminology

The fluid flow and heat transfer has a great role in the field of power producing units and plant. Hence the characteristics of fluid flow and heat transfer is needed to analysis for knowing the phenomena of system.

1.8.1 Heat transfer processes

It may be defined as "the transmission of energy from one region to another as a result of temperature gradient".

There are three mode of heat transfer-

(i) **Conduction-** Conduction is the transfer of heat from one part of substance to another part of the same substance. In solids it takes place by means of atomic vibration and movement of free electron.

Fourier's law states that "the rate of heat conduction is proportional to the area measured normal to the temperature gradient in that direction".

$$\boldsymbol{Q = -KA\frac{\partial T}{\partial x}} \qquad (1.1)$$

Where,

K = Thermal conductivity A= Area of heat transfer

$\frac{\partial T}{\partial x}$ = Temperature gradient

(ii) **Convection-** It is the heat transfer due to the temperature difference because of relative motion of the fluid over the surface. Convection is the possible only in the presence of fluid. Convection is occurs two type-

(a) **Free or natural convection-** Free or natural convection occurs when the fluid circulates by virtue of the natural differences in densities of hot and cold fluid. The denser portion of the fluid moves downward because of the greater force of gravity as compared with the force on less dense.

(b) **Forced convection -** When the works is done to blower or pump the fluid, it is said to be forced convection. The convection heat transfer may be expressed by Newton's law of cooling as follows;

$$\boldsymbol{Q = hA(T_s - T_f)} \qquad (1.2)$$

Where,

h = Coefficient of convective heat transfer

A= Area exposed to heat transfer

T_s= Surface temperature

T_f= Fluid temperature

(iii) **Radiation-** It is the transfer of heat in the form of electromagnetic wave. In radiation medium is not required.

Stefan-Boltzmann law- The law states that the emissive power of black body is directly proportional to fourth power of its absolute temperature.

$$\boldsymbol{Q = \sigma T^4} \quad (1.3)$$

Where,

σ = Stefan-Boltzmann constant and its value is $5.67 \times 10^{-8}\ W/m^2K^4$

T = Absolute Temperature

1.8.2 Fluid Flow Terminology

(i) **Laminar Flow -** Laminar flow is that type of flow in which the fluid particle moves along well-defined path or stream line and all stream line are straight and parallel. Thus the particle moves in laminas or layers gliding smoothly over the adjacent layer.

(ii) **Turbulent Flow** -Turbulent flow is that type of flow in which the fluid particle move in zig-zag way. Due to the movement of fluid particle in zig-zag way, the eddies formation place which are responsible for high energy loss.

(iii) **Viscosity -** It is the internal resistance offered by a layer of fluid to its adjacent layer against relative motion. Both liquid and gas viscosity is a function of temperature only. The dependence on pressure is negligible and with increase in temperature the viscosity of liquid is decreases and the viscosity of gas increases.

Table 1.1 Kinematic and Dynamic viscosity

Dynamic viscosity (μ)	For water is 1.002×10^{-3} Ns/m^2	For air is 1.814×10^{-5} Ns/m^2
Kinematic viscosity (ν)	For water is 1.04×10^{-6} m^2/s	For air is 1.67×10^{-5} m^2/s.

(iv) **Reynolds Number -** It is defined as the ratio of inertia force of flowing fluid and viscous force of the fluid. It is given by \

$$\boldsymbol{Re = \frac{\rho VD}{\mu}} \quad (1.4)$$

Where, ρ = Density of fluid V= Velocity of fluid

D= Characteristics dimension μ = Viscocity

(v) **Nusselt Number -** Nusselt Number is the dimensionless convection heat transfer coefficient and it is the ratio of convective heat flow to conductive heat flow.

$$\boldsymbol{Nu = \frac{hL}{k}} \qquad \textbf{(}1.5\textbf{)}$$

Where,

L = Characteristic length,

k = Thermal conductivity of the fluid,

h = Convective heat transfer coefficient of the fluid.

1.9 Concept of Boundary Layer - The concept of a boundary layer as proposed by Prandtl (1904) from the starting point for the simplification of the equation of motion and energy. It has been successfully used in many problems. In this concept the flow field over a body is divided into two regions-

(i) A thin region near the body, called the boundary layer, where the velocity and temperature gradient are large.

(ii) The region outside the boundary layer where velocity and temperature are very nearly equal to their free stream value.

The thickness of the boundary layer has been defined as the distance from the surface at which the local velocity (or temperature) reaches 99% of the external velocity (or temperature).

1.9.1 Velocity Boundary Layer - When real fluid flows past a stationary solid boundary, a layer of fluid which comes in contact with the boundary surface adheres to it and condition of no slip occurs. Thus the layer of fluid which can't slip away from the boundary surface undergoes retardation, this retarded layer further causes retardation of the adjacent layers of the fluid, thereby developing a small region in the immediate vicinity of the boundary surface in which the velocity of the flowing fluid increases rapidly from zero at the boundary surface and approaches the velocity of main stream. The layer adjacent to the boundary is called boundary layer as shown in Fig.1.1.

1.9.2 Thermal Boundary Layer - Thermal boundary layer will develop if the surface temperature and free stream temperature are different. Whenever a flow of fluid takes place past a heated or cold surface, a temperature field is set up in the field next to the surface. If the surface of the plane is hotter than fluid the temperature gradient occurs due to the exchange of heat between

the plate and the fluid. The zone or layer where in the temperature field exists is called thermal boundary layer as shown in Fig.1.2.

1.9.3 Viscous Sub Layer - If the plate is very smooth, even in the region of turbulent boundary layer, there is a very thin layer just adjacent to the boundary in which the flow is laminar as shown in Fig. 1.1. This thin layer is commonly known as laminar sub layer.

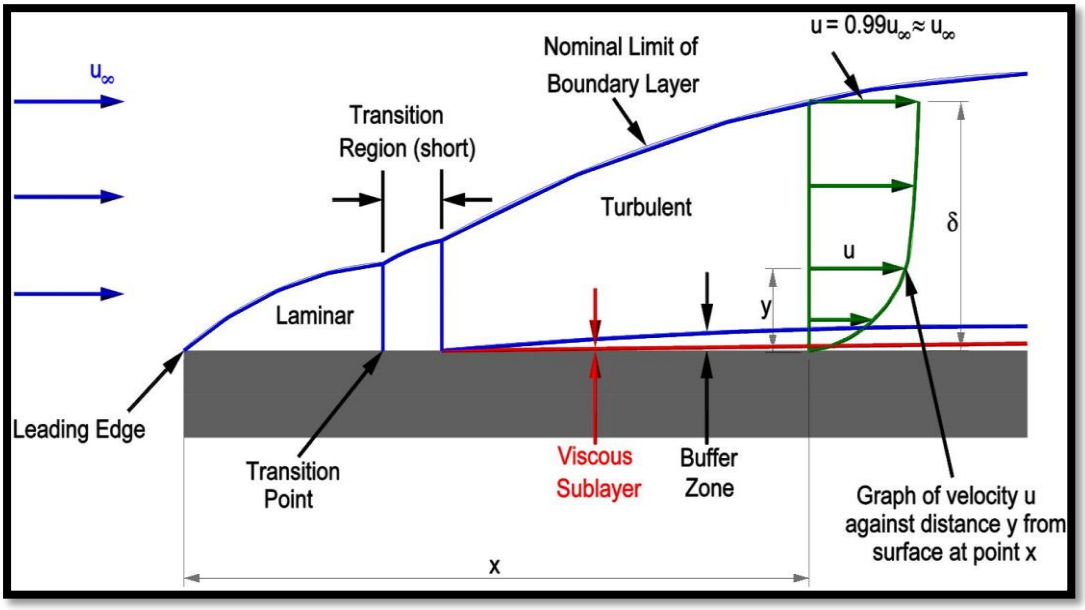

Fig.1.1 Development of velocity boundary layer on a flat plate

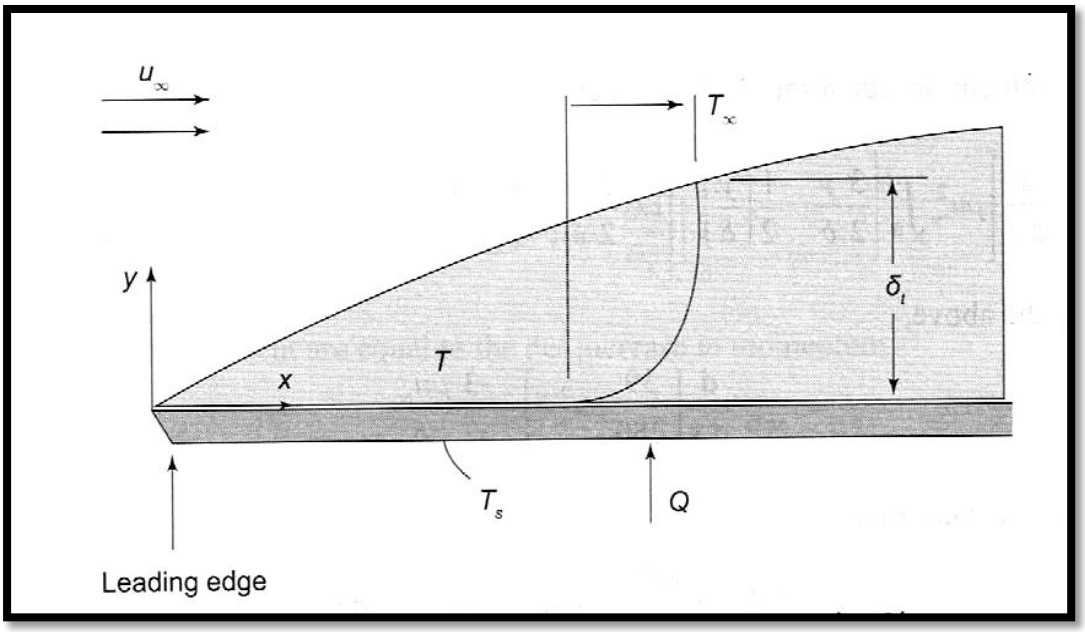

Fig. 1.2 Thermal boundary layer

CHAPTER -2

SOLAR COLLECTOR

2.1 Introduction

A solar collector collects heat by absorbing sunlight. Solar radiation is energy in the form of electromagnetic radiation from the infrared (long) to the ultraviolet (short) wavelengths. The quantity of solar energy striking the Earth's surface (solar constant) averages about 1,000 watts per square meter under clear skies, depending upon weather conditions, location and orientation.

2.2 Types of Solar Collectors

1. Flat plate type solar collectors
    a. Solar water heater or Liquid heating collector
    b. Solar air heater
2. Concentrating type solar collectors
    a. Cylindrical parabolic concentrating solar collector
    b. Compounded parabolic concentrating solar collector
    c. Paraboloidal dish concentrating solar collector

2.2.1 Flat plate type solar collectors

Flat plate solar collectors are the most common type of solar collectors for solar water heating system and solar space heating system. A typical flat-plate collector is an insulated metal box with a one or two glass or plastic cover (called Glazing) and a dark colored absorber plate. These collectors heat liquid or air at temperature less than 82.2^0C. It is designed for a variety of applications in which temperature ranging from ambient to 100^0C. It is the most important type of solar collector because it is simple in design, cheap in construction and easy in operation.

Components of flat-plate solar collector

(i) **Absorber Plate -** Absorber plate generally made from metal i.e. aluminum, copper, G.I. sheet and steel. Absorber plate thickness ranging from 0.2 to 2 mm and surface is coated black in color to absorbed more radiation.

In absorbing surface,

Absorptivity (α) = 1 Reflectivity (ρ) = 0 Transmissibility (τ) = 0

(ii) **Transparent Covers -** A transparent covers which may be of glass 4 to 5mm thick or radiation transmitting plastic sheet. Transparent glass cover is used as it allows shorter wavelength radiation to pass and restricts larger wavelength radiation to go back. This increases the temperature of absorber plate.

In transparent covers,

Absorptivity (α) = 0 Reflectivity (ρ) = 0 Transmissibility (τ) = 1

(iii) **Duct or passages -** There is passage between absorber and bottom surface through which air flows called as ducts as shown in Fig. 2.1

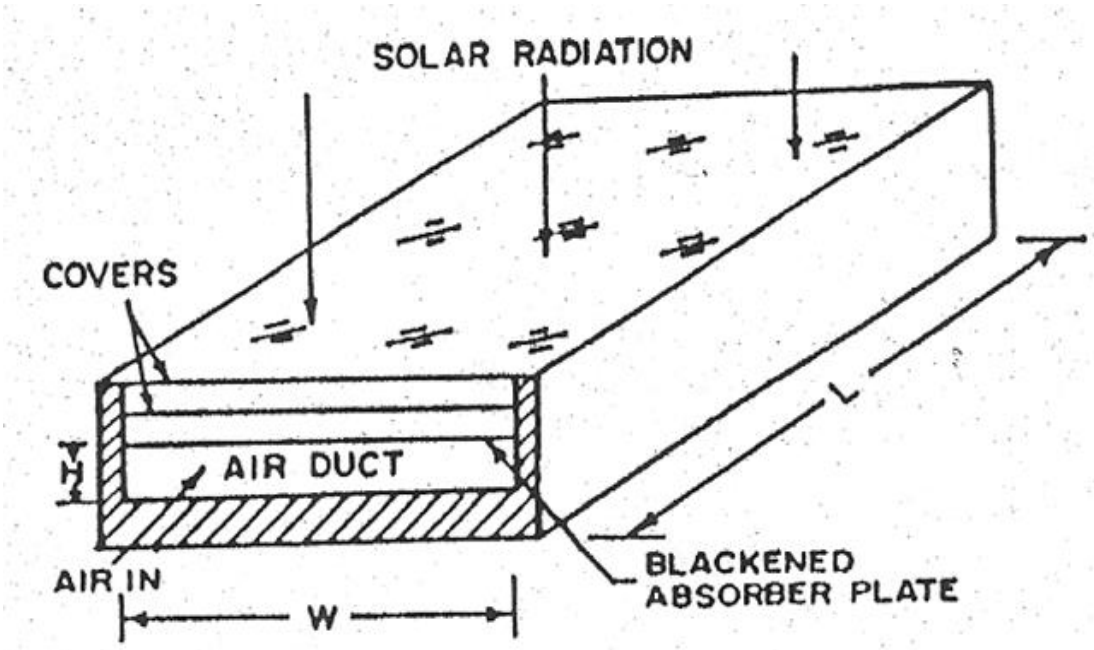

Fig. 2.1 Solar air heater duct

(iv) Insulation - Restriction to heat flow is termed as insulation. Insulation should be provided at the back and sides to minimize heat losses.

(v) Housing - The collector housing is used to protect the insulation and absorber plate from the environment. It also provides collector mountings. Various metals (aluminium, galvanized steel), fibre-glass or high temperature plastics are commonly used. Wood has also been in a few housings. When metal is used, correction can be a problem.

(vi) Seals - At least two pipes or ducts pass through openings in the housing. It is essential that these openings be sealed to prevent dust from entering the collector. Any dust in the

collectors will partially deposit on the absorber surface and reduce its absorbance. The seals must also block rain or snow, both of which can deteriorate the insulation, the absorber plate, and even the collector housing.

Types of flat plate solar collectors

(a) Solar Water Heater

It is a flat-plate fin tube collector. A number of tubes integral with the collector absorber plate or connected to it carry the water to be heated. The absorber, whose sun facing surface is blackened, absorbs heat incident solar radiation and transfer the heat to the water flowing in the tubes. One or more of glass or plastic covers reduce the thermal losses from the unit. These covers are transparent to the short wave solar radiation but opaque to the long wave (heat) radiation of the absorber plate and thus reduce the radiation losses to the atmosphere. In addition, convection losses are also reduced by covers. The back and edges of the collectors are also properly insulated. Fig. 2.2 shows the solar water heater.

(b) Solar Air Heater

The conventional solar air heaters mainly consist of a panel, insulated hot air ducts and air blowers if it is an active system. The panel consists of an absorber plate thermally insulated from the bottom, the sides are also insulated, and a glass or plastic cover is fixed above the absorber plate forms a passage for air flow. These covers are transparent to the short wave solar radiation but opaque to the long wave (heat) radiation of the absorber plate and thus reduce the radiation losses to the atmosphere. The air to be heated is passed through a duct below blackened light gauge steel or aluminum or G.I. sheet absorber plate with the help of blower or fan. In some designs the air flow above the absorber plate. Proper insulation is also provided on the back and edges side. Fig. 2.3 shows the solar air heater.

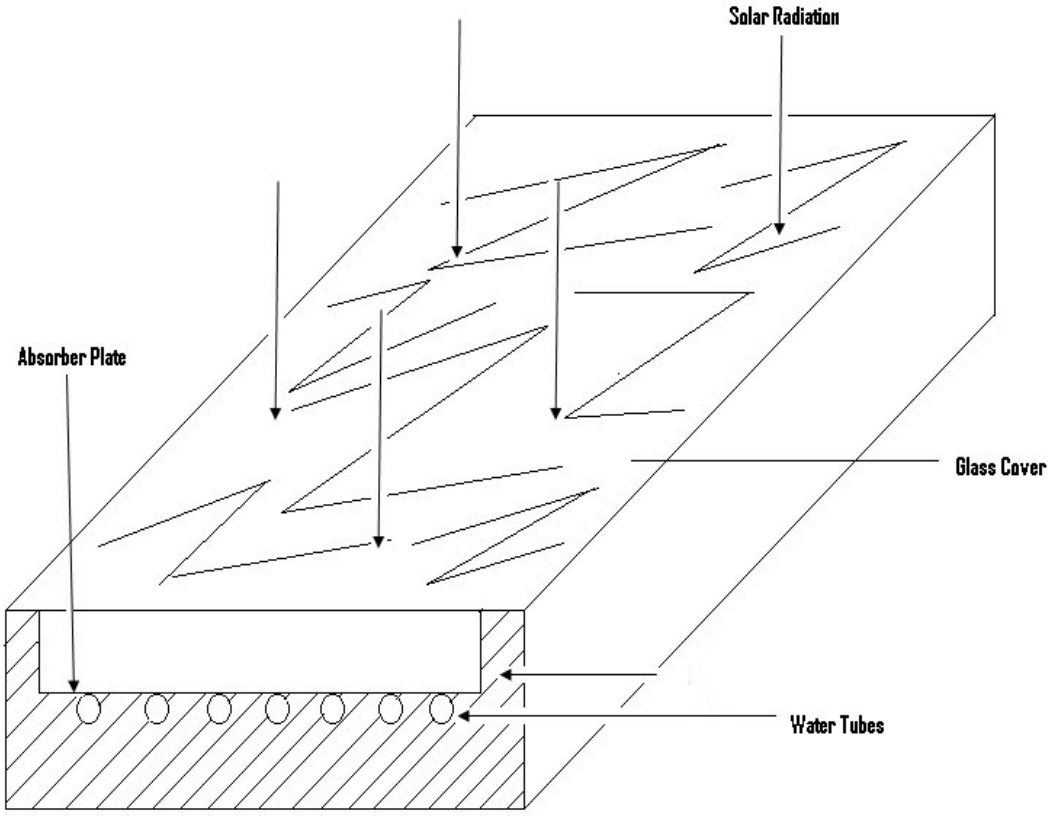

Fig. 2.2 Solar Water Heater

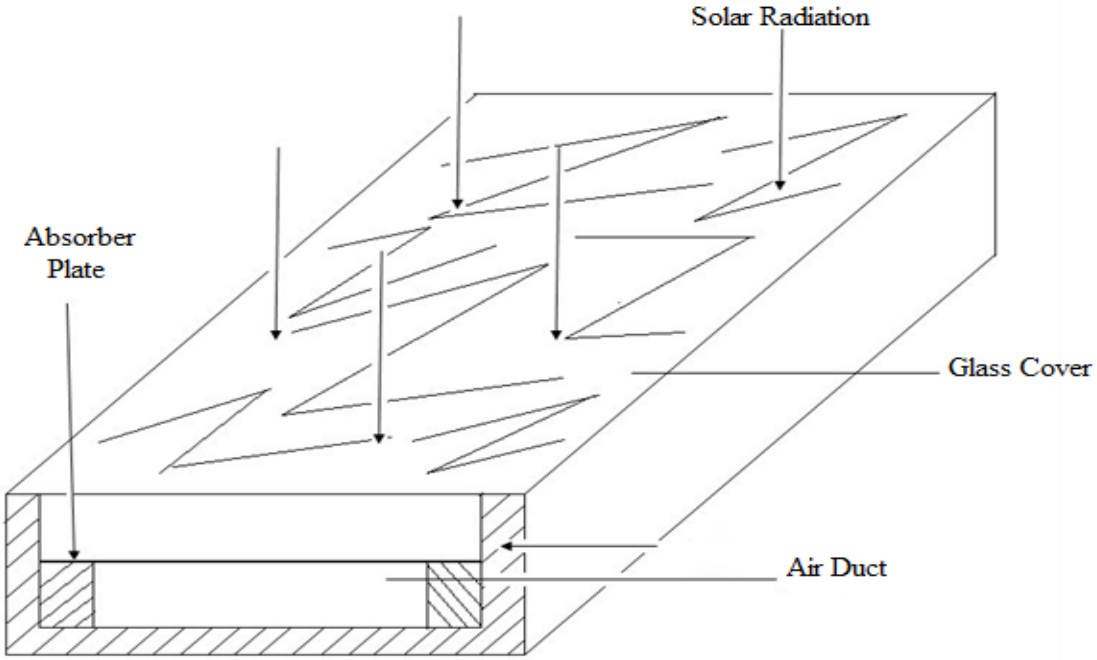

Fig. 2.3 Solar Air Heater

2.2.2 Concentrating Type Solar Collectors

Concentrating or focusing collectors intercept direct radiation over a large area and focus it on small absorber area. It can provide high temperature more efficiently than flat-plate collectors, since the absorption surface area is small. However, diffused sky radiation cannot be focused on the absorbing surface. Most concentrating collectors require mechanical equipment that constantly orients the collectors toward the sun and keeps the absorber at the point of focus.

Type of concentrating type solar collectors-

(a) Compounded parabolic concentrator solar collector

In a compounded Parabolic Concentrator two parabolic reflector are attached to a flat plate receiver. Parabolic reflector is arranged in such a way that, the focus of one is located at the bottom end point of the other. Thus solar radiation from many directions is reflected toward the bottom of through. Due to this characteristic a compounded Parabolic Concentrator can collect large proportion of solar radiation, including both direct and diffused radiation concentrated on a small area. It has a large acceptance angle about 11.5°, and need to adjust regularly. The concentration ratio of this collector is in the range of 3-10. The Compounded parabolic concentrator is shown in Fig.2.4

(b) Cylindrical parabolic concentrator solar collector

In this collector the reflector is in the form of trough with a parabolic cross section in which the image is formed on the focal line on the parabola. The absorber tube is polished black at the outer surface to increase absorption. The heat transfer fluid flow through the receiver tube and transfer the thermal energy to the next stage of the system. The collector can be oriented in any of the three direction i.e., east-west, north-south or polar. However, the polar configuration gives the better performance. These collectors can provide concentration ratio in the range of 10-30. The Cylindrical parabolic concentrator is shown in Fig.2.5

(c) Paraboloidal dish concentrating solar collector

In paraboloidal dish concentrating solar collector the solar radiation to focus at a point the dished can be turned automatically about two axes (up-down and left- right) so that the sun is always kept in a line with the focus and the base of the paraboloidal dish. The absorber located at the focus, is the cavity made of a zirconium-copper alloy with a selective coating of black chrome. A commercially used parabolic dish collector is of 6 m in diameter constructed from

200 curved mirror segments forming a paraboloid surface. The Paraboloidal dish concentrator is shown in Fig.2.6

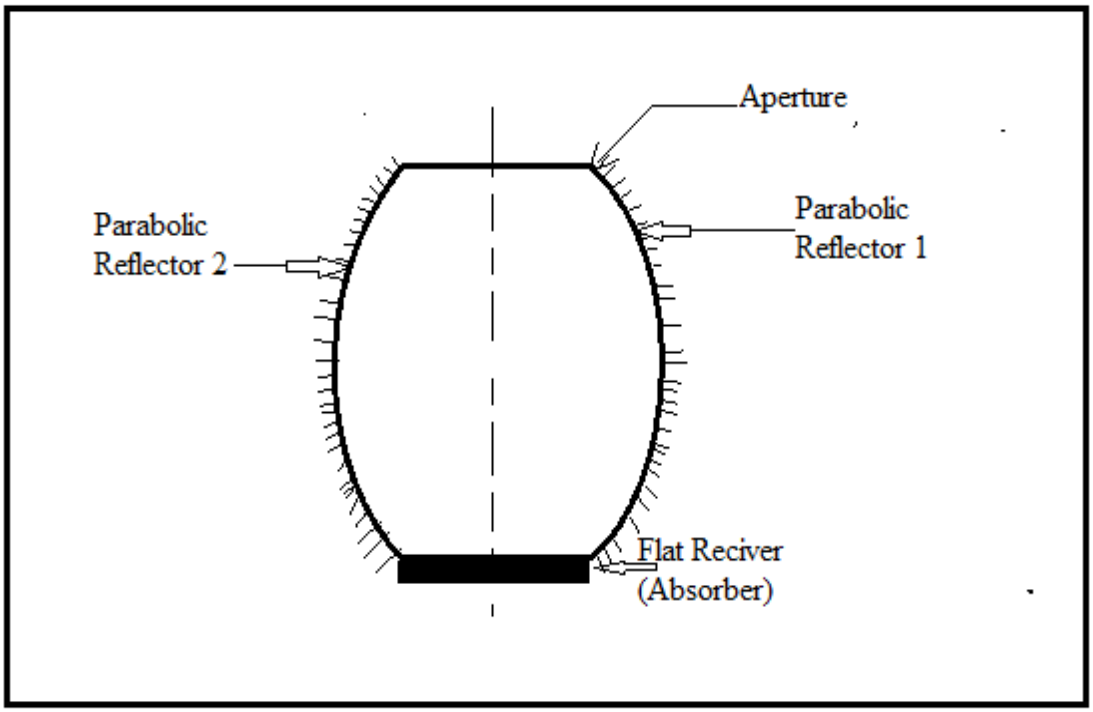

Fig. 2.4 Compounded parabolic concentrator

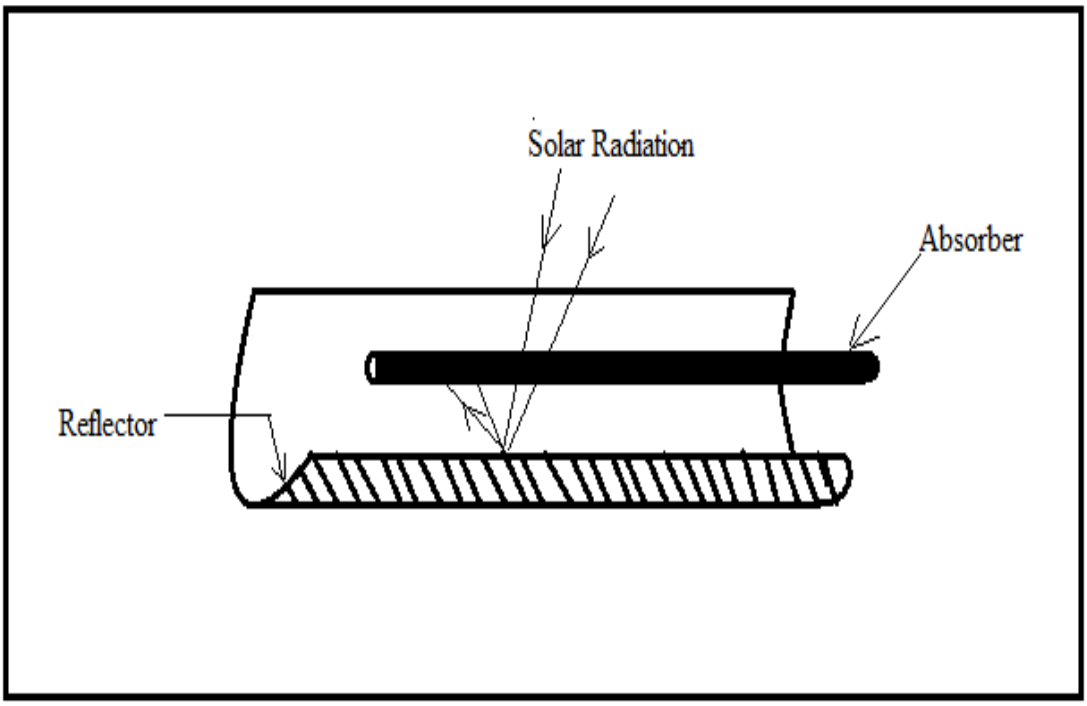

Fig. 2.5 Cylindrical parabolic concentrator

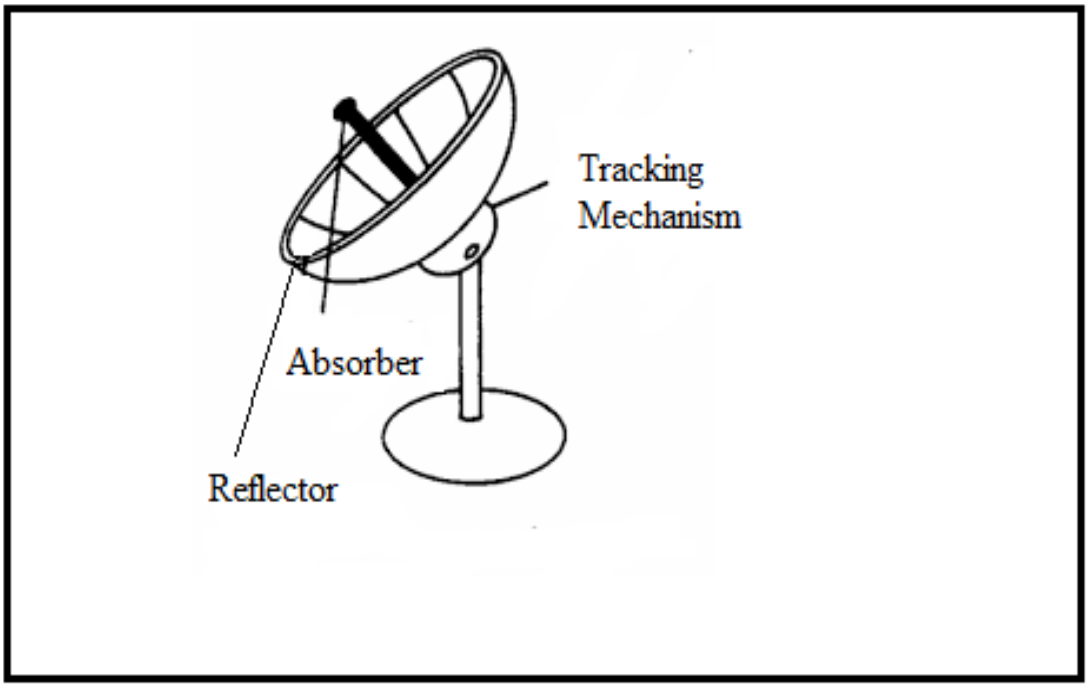

Fig. 2.6 Paraboloidal dish concentrator

2.3 Types of Air Heating Collector

As shown Fig. 2.7 air is generally used as a heat transfer fluid in many types of energy conversion system. In drying application and for heating of buildings.

(i) **Simple flat-plate collector -** This is the simplest and most commonly used type of collector. In its simplest form it is composed of one or two glazings over a flat plate backed by insulation. The path of air flow may be either above or below or the absorber plate.

(ii) **Finned-plate collector -** This is a modified version of the type (i) collector, where the heat transfer co-efficient is increased by using fins on the flat plate absorber, and in certain design the surface is made directionally selective. The fins are usually located in the air-flow passage.

(iii) **Corrugated- plate collector -** This is another variation of the simple flat-plate design, in which the absorber is corrugated either in rounded troughs or V-troughs. This increases the heat transfer area and may make the surface directionally selective.

(iv) **Matrix type collector -** In this design an absorbing matrix is plate, cotton gauze or loosely packed porous material. This type of collector offers a high heat-transfer to volume ratio; it may also offer low friction losses depending on the design.

(v) **Overlapped transparent plate type collector -** This type of collector is composed of a staggered array of transparent plates which are partially blacked. The air flow paths are between the overlapped plates.

(vi) **Transpiration collector** - The transpiration or porous bed design is a variation of type (iv), in which the matrix material is closely packed and the backed and the back absorber-plate is eliminated. The air flow usually enters just under the innermost cover and flows downward through the porous bed and into the distribution ducting.

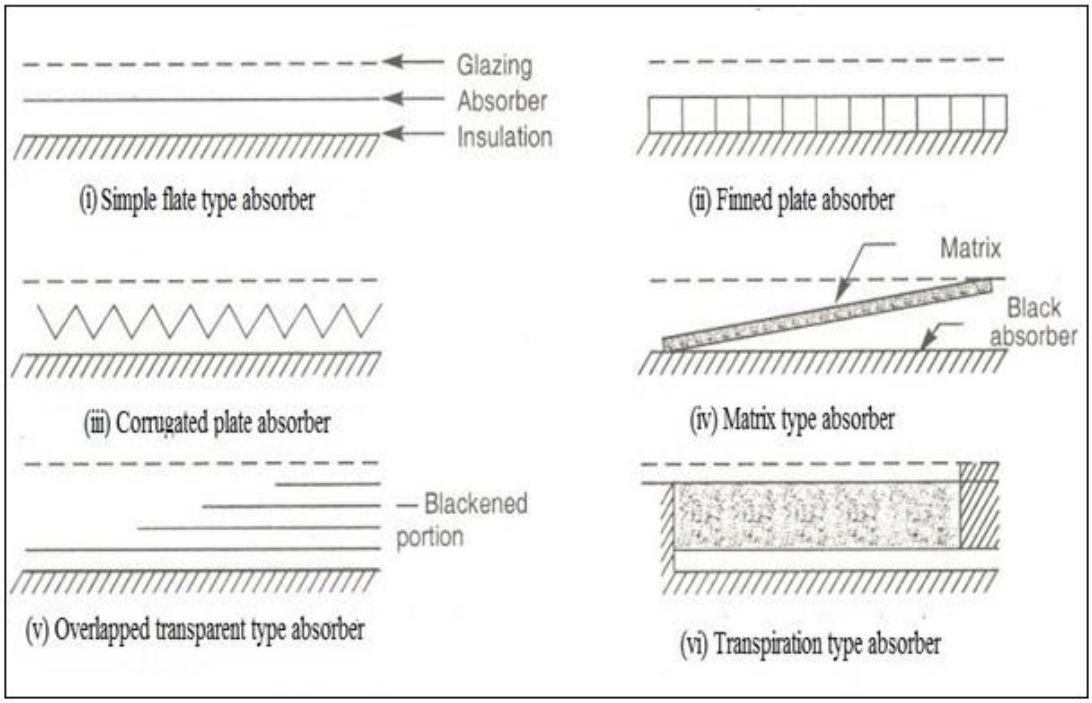

Fig.2.7 Various types of air heaters according to the absorbing surface

2.4 Collector Performance

Several investigators have analyzed thermal performance of flat-plate solar air heaters. The thermal performance of the solar air heater is described by an energy balance, which indicates the distribution of incident solar energy into useful energy gain (Q_u) and various losses (Q_L) as shown in fig. 2.8.

The detail of the performance analysis of a solar collector is given below. Energy balance on the collector can be written as;

$$A_c[1R(\tau\alpha)] = Q_u + Q_L \qquad (2.1)$$

The useful energy "Q_u" can be written in the terms of known temperature "T_i" and other system and operating parameters as;

$$Q_u = A_c F_R [S - U_L (T_i - T_a)] \quad (2.2)$$

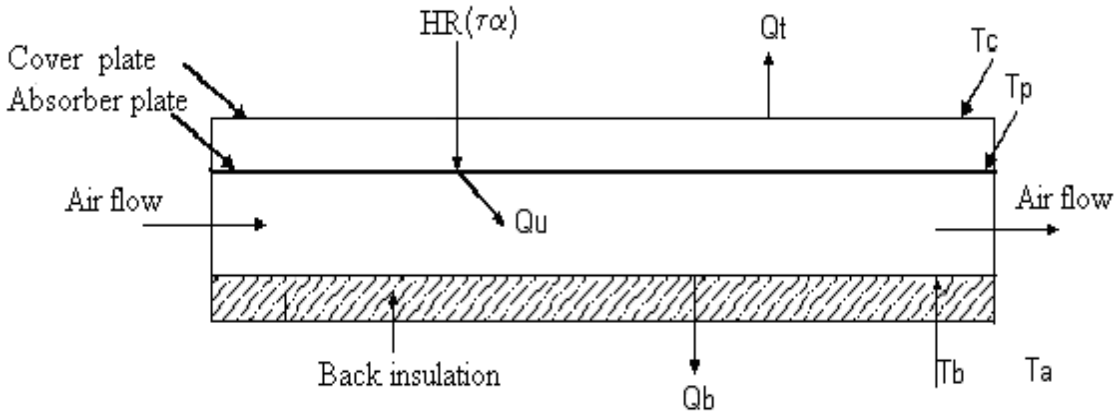

Fig.2.8 Energy Balance of Collector

The thermal efficiency of a collector can be written as;

$$\eta_{th} = F_R \left[(\tau\alpha) - U_L \left(\frac{T_i - T_a}{I}\right)\right] \quad (2.3)$$

The heat removal factor can be expressed as;

$$F_R = \frac{GC_p}{U_L}\left[1 - exp\left(\frac{-F_P U_L}{GC_P}\right)\right] \quad (2.4)$$

Where, F_p is the collector efficiency factor defined as the ratio of actual useful heat collection rate to that attainable with entire absorber plate at average fluid temperature.

The collector efficiency factor for solar air heater can be expressed as;

$$F_P = \frac{h}{h + U_L} \quad (2.5)$$

A Parameter F'', known as flow factor is defined as follows;

$$F'' = \frac{GC_P}{U_L F_P}\left[1 - exp\left(\frac{-F_P U_L}{GC_P}\right)\right] \quad (2.6)$$

Knowing the value of factor F_R, $F''$and other parameters the mean fluid temperature T_f and the mean plate temperature $T_P$can be calculated from the following equations.

$$T_f = T_i + \left[\frac{Q_u/A_C}{U_L F_R}\right](1 - F'') \quad (2.7)$$

$$T_P = T_i + \left[\frac{Q_u/A_C}{U_L F_R}\right](1 - F_R) \quad (2.8)$$

The air heater performance was computed for the most useful range of design and working conditions. In particular condition of a solar air heater drawing air from the atmosphere, the inlet air temperature coincides with the ambient and the Eq.(2.9) then reduces to,

$$\eta_{th} = F_R(\tau\alpha) \quad (2.9)$$

This expression of efficiency does not allow the real operative temperature to be shown. In view of these limitations, the following equation for the efficiency of the solar air heater has been proposed [1].

$$\eta_{th} = F_O\left[(\tau\alpha) - U_L\left(\frac{T_O - T_i}{I}\right)\right] \quad (2.10)$$

Where, F_o is the heat removal factor referred to outlet air temperature and is expressed as;

$$F_O = \frac{GC_P}{U_L}\left[exp\left(\frac{F_P U_L}{GC_P}\right) - 1\right] \quad (2.11)$$

Further, performance can also be expressed by another equation, containing temperature gain by the fluid flowing through the collector as given below;

$$\eta_{th} = GC_P\left[\frac{T_O - T_i}{I}\right] \quad (2.12)$$

2.5 Applications of Solar Air Heater

(i) Heating building for comfort

(ii) Drying agricultural products

(iii) Heating green houses

(iv) Seasoning of timber, and

(v) Curing of industrial products such as plastics

2.6 Advantages of Solar Air Heater

(i) They have the advantage of using both diffuse and beam radiation

(ii) They do not require orientation towards the sun

(iii) They require little maintenance, and

(iv) They are mechanically simpler than the concentrating reflectors, absorbing surfaces and orientation devices of focusing collectors

2.7 Limitation of Solar Collector

(i) Solar air heaters have low thermal efficiency because of low convective heat transfer coefficient between the air and the absorber plate which leads higher temperature to the absorber plate and causes maximum thermal losses.

(ii) It has been found that the main thermal resistance to heat transfer from absorbing plate to fluid (air) flowing is due to formation of laminar sub layer on the heat transferring surface that need to be broken to increase heat transfer.

CHAPTER – 3

LITERATURE REVIEW

3.1 Review of Double Pass Solar Air Heater

The conventional solar air heaters mainly consist of a panel, insulated hot air ducts and air blowers if it is an active system. The panel consists of an absorber plate thermally insulated from the bottom, the sides are also insulated, and a glass or plastic cover is fixed above the absorber plate forms a passage for air flow. Hence, the major heat losses from flat-plate solar collectors are through the top cover as the bottom and the sides of the collector are very well insulated. The solar collector heat losses and heat transfer coefficient inside the solar collector are the two important parameters affecting the efficiency of the collector. In order to minimize the heat losses and to improve the efficiency, double glazing was advocated by some researchers [13]. It has been also suggested to insert an absorbing plate into a panel to have a double pass channel where the air flows from above and then below the absorber plate [11,12] or vice versa [17,19]. Esen [18] and Ozgen at al. [20] suggested passing the air from above and below the absorber plate at the same time in a double-flow solar air heater**.** The double pass counter flow arrangement with artificial roughness in the second air passage is one of the effective alternatives to improve its thermal performance.

Satccunanathan and Deonarine have suggested the use of two pass solar air heater in order to reduce the losses from the top. They constructed a unit in which the air first between the cover of the two glass cover heater and under the absorber plate. When operated as an open system with inlet air at ambient temperature. It was found that the outer glass cover temperature was lowered by 2 to 5 °C and that operated near the ambient temperature. As a result losses were reduced and the efficiency of the collector was measured to be 10 to 15% higher than of a conventional heater [16]. The schematic diagram is shown in figure 3.1

3.2 Review of Roughness Geometries

3.2.1 Artificial roughness

The application of artificial roughness is one of the promising techniques to enhance the heat transfer rate between absorber plate and air due to high effective heat transfer area per unit volume in solar air heater duct, resulting in high heat transfer capability. Providing metal ribs on absorber plate for the enhancement of heat transfer rate is due to the breaking of laminar sub layer and creating turbulence adjacent to the wall. However it also enhances the friction

factor therefore the geometry of the artificial roughness has selected in such a way that it create the turbulence with minimum pressure drop in solar air heater duct.

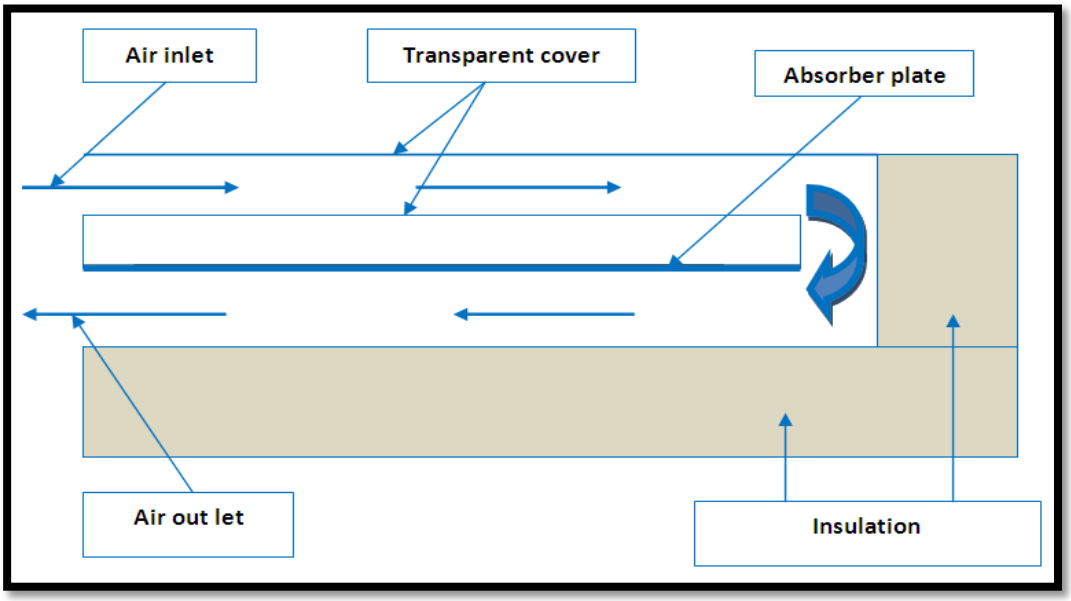

Fig.3.1 Schematic view of a double pass solar air heater

3.2.2 Basic terminology used in artificial roughness

(i) **Relative roughness pitch (p/e):** It the ratio of distance between two consecutive ribs and height of the rib.

(ii) **Relative roughness height (e/D):** It is the ratio of rib height to equivalent diameter of the air passage.

(iii) **Angle of attack (α):** Angle of attack is defined as the inclination of rib with direction of air flow in the duct.

(iv) **Aspect ratio:** Aspect ratio is defined as the ratio of duct width to duct height.

(v) **Shape of roughness element:** The common shape of roughness element is Square, circular, semi-circular, arc shaped wire, dimple or cavity, compound rib-grooved, and v-shaped continuous or broken ribs with or without gap.

Gupta et al. [1997] Performed an experiments on fluid flow and heat transfer characteristics of artificially roughened solar air heater ducts with inclined ribs. It was reported that with increase in relative roughness height (e/D) the value of Reynolds number (Re) decreased for which effective efficiency was maximum. The maximum heat transfer and friction factor were found at angle of attack of 60° and 70°, respectively in the range of parameter investigated. Inclined ribs enhance the heat transfer more than the transverse rib due to generation of secondary flow in

addition to breaking the laminar sub layer which leads to the creation of high heat transfer region at the leading edge of the rib [1]. The investigated geometry has been shown in Fig. 3.2

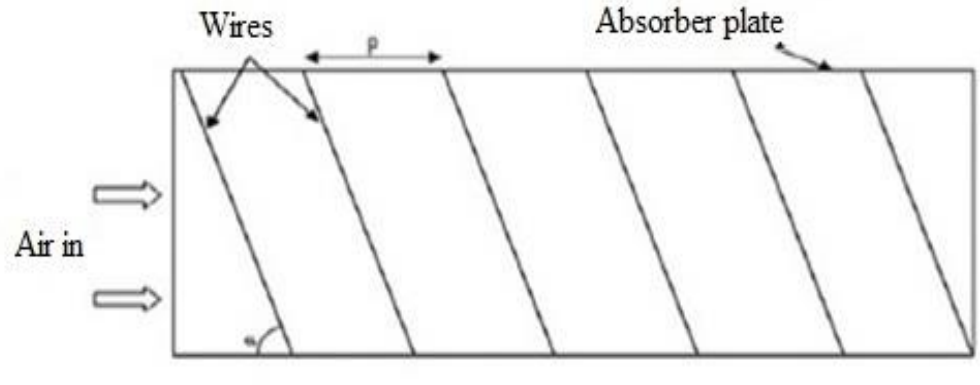

Fig.3.2 Inclined ribs

Varun et al. [2008] investigated the thermal performance of solar air heater having roughness geometry as combination of inclined as well as transverse rib. They used the performance Parameter like as Reynolds number (Re) ranges from 2000-14000, Relative roughness pitch (p/e) of 3-8 and Relative roughness height (e/D) of 0.030. It was observed that the optimum thermal performance occurs having the value of Relative roughness pitch (p/e) of 8 [2]. The investigated geometry has been shown in Fig.3.3

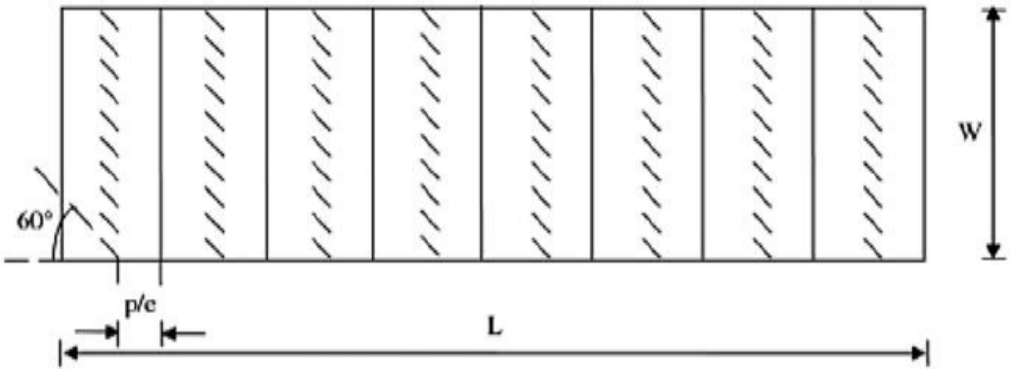

Fig.3.3 Inclined and transverse ribs

Prasad and Saini [1998] used roughness geometry in the form of transverse continuous ribs on the absorber plate and studied the effect of roughness and flow parameter such as relative roughness height (e/D) and relative roughness pitch (p/e) on heat transfer and friction factor. They developed expressions for the heat transfer and friction factor for a fully turbulent flow. It was observed that maximum heat transfer occurred in the vicinity of reattachment points [3]. The investigated geometry has been shown in Fig.3.4

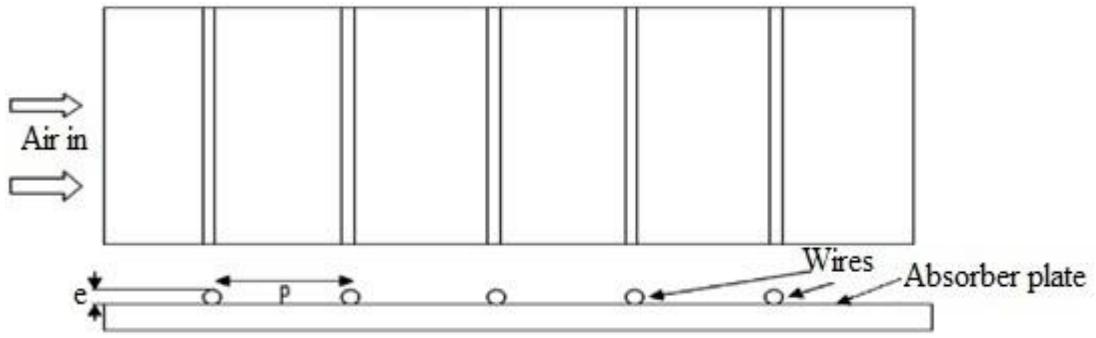

Fig.3.4 Transverse continuous ribs

Sahu and Bhagoria [2005] investigated the effect on the thermal Efficiency of solar air heater and heat transfer coefficient by providing 90^0 broken transverse ribs on absorber plate. They used the performance parameter likes height of rib (e) 1.5mm, pitch (p) 10-30mm, Reynolds number (Re) 3000-12000, Relative roughness height (e/D) is 0.338 and duct ratio (W/H) is 8. The maximum enhancement of heat transfer coefficient occurs at pitch of about 20mm. It was reported that, heat transfer coefficient and maximum thermal efficiency obtained as 1.25 to 1.4 times and 83.5% than that of smooth duct respectively [4]. The investigated geometry has been shown in Fig.3.5

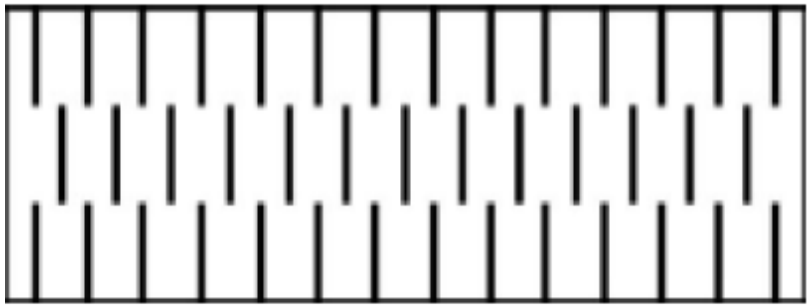

Fig.3.5 Transverse broken ribs

Momin et al. [2002] experimentally investigated the effect of geometrical parameters of V-shape ribs on heat transfer and fluid flow characteristics of a rectangular duct of a solar air heater. The investigation covered a Reynolds number (Re) range of 2500–18000, relative roughness height (e/D_h) of 0.02–0.034 and angle of attack of flow (α) of 30–90° for a fixed relative pitch of 10. It was found that for angle of attack (α) of 60° in the v- shaped rib enhanced the value of Nusselt number by 1.14 and 2.30 times and friction factor by 2.30 and 2.38 over inclined ribs and smooth plate[5]. The investigated geometry has been shown in Fig.3.6

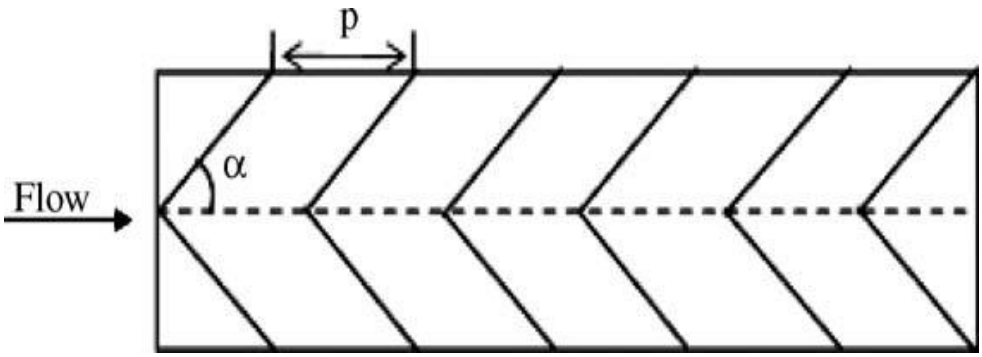

Fig.3.6 V-Shape ribs

Singh et al. [2011] experimentally investigated the effect on heat transfer and friction in rectangular ducts roughened with a new configuration of discrete v-rib on the absorber plate. The maximum enhancement in Nusselt number and friction factor has been obtained at relative gap position of 0.65 and is of order of 2.8 and3.0 times of that of the smooth duct, respectively [6]. The investigated geometry has been shown in Fig.3.7

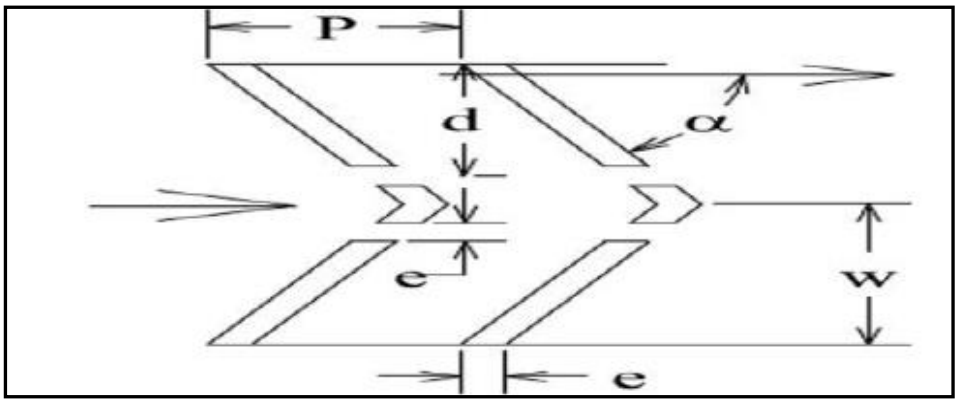

Fig.3.7 Inverted -V -discrete ribs

A Lanjewar at al. [2011] experimentally investigated heat transfer and friction factor in solar air heater with different orientation of W-Rib roughness. W rib have been tested both pointing in downstream W-down and upstream W-up to the flow. The parameter is taken by this Reynolds number 2300-14,000, aspect ratio (W/H) of 8, relative roughness pitch (p/e) of 10, relative roughness height (e/D_h) of 0.03375 and the angle of attack (α) of 30-75°. W-down ribs give better thermo-hydraulic performance than W-up and V-ribs. Maximum thermo-hydraulic performance for W-down rib is 1.98 and W-up rib is 1.81[7]. The investigated geometry has been shown in Fig.3.8

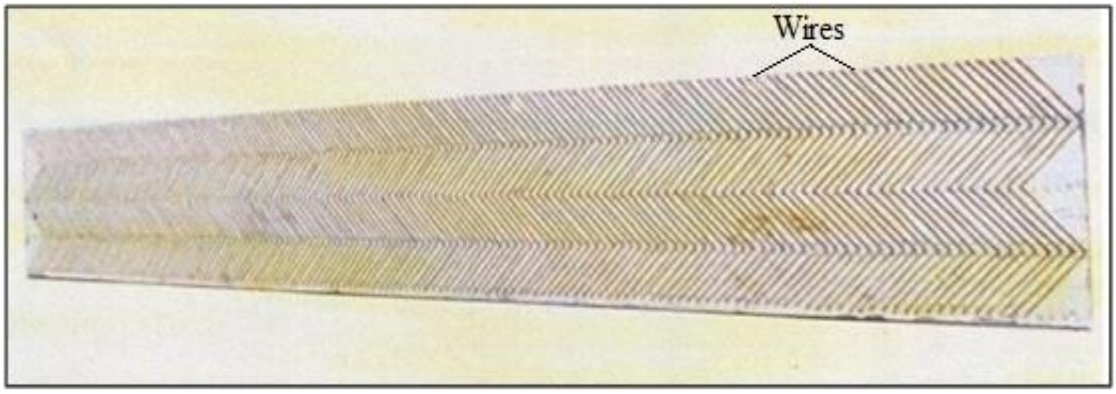

Fig.3.8 W-down roughness geometry

Kumar et al. [2008] experimentally investigated to determine the heat transfer distributions in solar air heater having its absorber plate roughened with discrete W-shaped ribs. The experiment encompassed Reynolds number (Re) range from3000 to 15,000, rib height (e) values of 0.75 mm and 1 mm, relative roughness height (e/D) 0.0168 and 0.0225 and relative roughness pitch (p/e) of 10 and angle of attack (a) 45°. Thermal performance of roughened solar air collector was compared with that of smooth one under similar flow conditions and it was reported that thermal performance of the roughened channel was 1.2–1.8 times the smooth channel for range of parameters investigated [8]. The geometry investigated has been shown in Fig.3.9

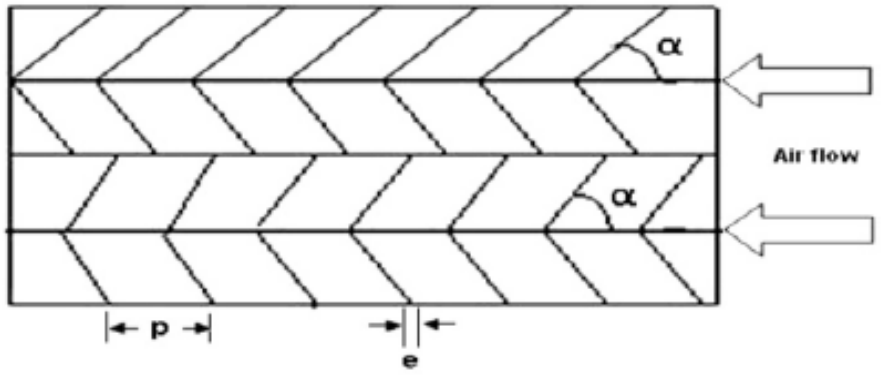

Fig.3.9 Discrete W-shaped ribs

Jaurker et al. [2006] experimentally investigated the effect of artificial roughness by provide rib-grooved geometry on the inner surface of absorber plate of solar air heater. The experimental investigation encompassed the Reynolds number range from 3000 to 21,000, relative roughness height 0.0181–0.0363, relative roughness pitch 4.5–10.0, and groove position to pitch ratio 0.3–0.7. The optimum condition for heat transfer occurs at a groove position of 0.4, when the relative roughness pitch (p/e) is about 6. It has also been observed that as compared to smooth duct, the pressure of rib grooved artificial roughness increase the Nusselt number up to 2.75 times, while

the friction factor raised up to 3.61 times in the range of parameters investigated [9]. The geometry investigated has been shown in Fig.3.10

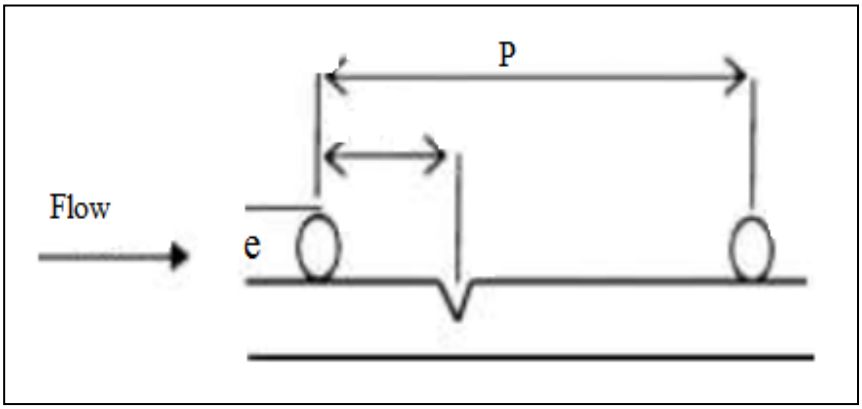

Fig.3.10 Rib-groove geometry

Saini and Saini [1997] experimentally investigated on the effect of wire mesh roughened absorber plate on heat transfer augmentation and friction characteristics of solar air heater. The investigation considered relative long way length of mesh (L/e) in range of 25–71.87, relative short way length of mesh (S/e) in range of 15.62–46.87, relative roughness height (e/D) in range of 0.12–0.039 and Reynolds number (Re) in range of 1900–13,000. It was reported that the maximum heat transfer of order 4 times over the smooth duct [10]. The geometry investigated has been shown in Fig. 3.11

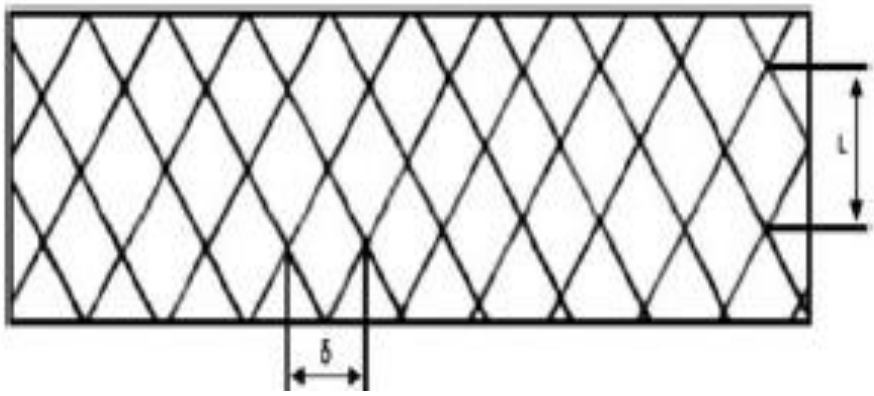

Fig.3.11 Expanded wire mesh fixation

Aharwal et al. [2008] experimentally investigated the effect of artificial roughness by inclined split rib arrangement in a rectangular duct in solar air heater .The duct had an aspect ratio (W/H) of 5.84, relative roughness pitch (p/e) of 10, relative roughness height (e/D) of 0.0377, angle of attack (α) of 60, relative gap width (g/e) range of 0.5–2 and relative gap position (d/W) varied from 0.1667 to 0.667 for Reynolds number (Re) range of 3000– 18,000. For the split-rib and continuous rib roughened ducts, the enhancement in heat transfer was reported to be in the range

of 1.71–2.59 and 1.48–2.26 times respectively over smooth duct under similar operating conditions [21]. The investigated geometry has been shown in Fig.3.12

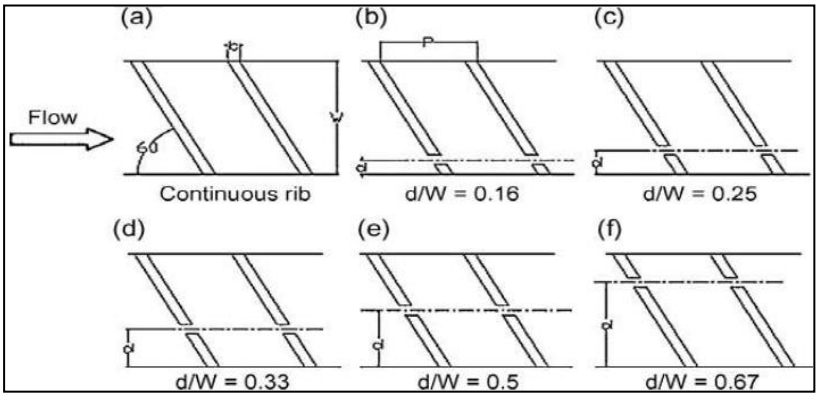

Fig.3.12 Inclined with gap ribs

J.S.Saini et al [2011] experimentally investigated the effect of heat transfer and friction factor correlation of solar air heater with discrete V-down ribs on absorber plates. The parameters are Reynolds number (Re) range of 3000-15000, relative roughness pitch (p/e) range of 4- 12, angle of attack (α)range of 30° to 75°, relative gap position (g/e) range of 0.5- 2.0 and relative roughness height (e/D_h) range of 0.015- 0.043 has been found that, the maximum increase in Nusselt no. and friction characteristics is 3.04 and 3.11 times higher to that of smooth duct and The maximum value of Nusselt number and friction occurs at relative roughness pitch of 8[22]. The investigated geometry has been shown in Fig.3.13

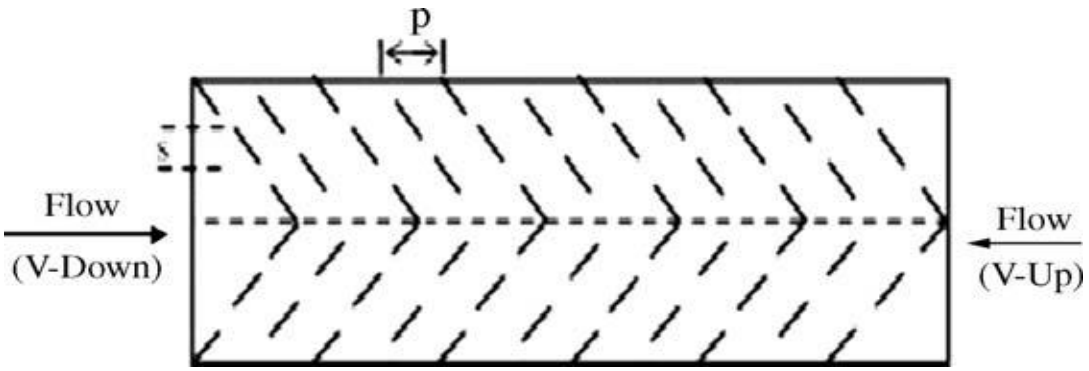

Fig.3.13 Discrete V- down ribs

CHAPTER – 4

EXPERIMENTAL INVESTIGATION

As per the literature review in chapter 3 it is found that it is necessary to design, develop and fabricate the double pass solar air heater duct as per specification given in literature review.

4.1 Experimental Set up

An experimental setup has been designed and fabricated [2l] to18mm thick wooden ply with 12mm thick insulation around rectangular outlet. The enhancement of heat transfer having multi v-shaped ribs with gap made from G.I. wires of 16 gauges, on the G.I absorber Rectangular plate of 22 gauges. The flow of entry section (400mm×200mm), test section (1500mm×200mm), exit section (200mm×200mm) respectively as recommended in ASHRAE standards 93-77[15]. A 25 mm cotton wool of thermal conductivity 0.029W/ m K was applied as insulation and flow measuring orifice plate (25mm) and a centrifugal blower (3-phase, 440 V, 3.0 kW and 2880 r.p.m.AC motor) with a control valve. The mass flow rate of the air is measured by means of an orifice plate connected with a U-tube manometer with distilled water as manometric fluid and flow is controlled by the control valve provided in the pipe line.

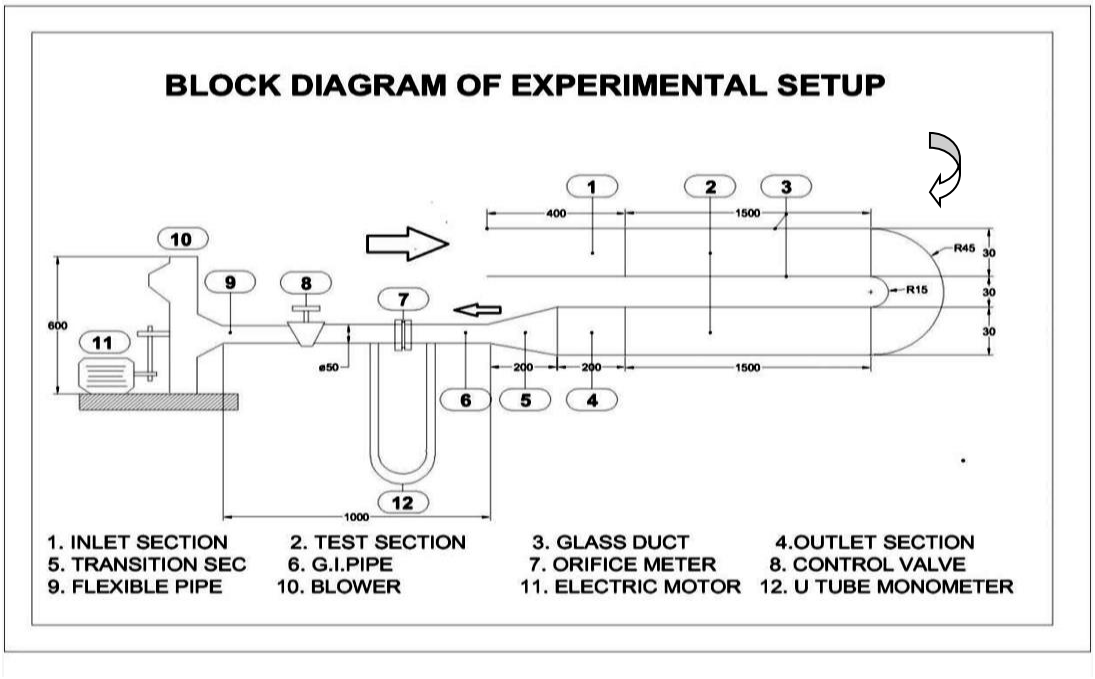

Fig.4.1 (a) Experimental setup block diagram

The air enters at entry section and first pass section where the atmospheric air slightly preheated by trapped heat between two transparent glass cover and then enter in to test section

where that preheated air gets heated by taking heat from absorber G.I. plate of 22 ASWG of (1500mm×200mm) which gets it heat from electric heater of uniform heat flux up to a maximum of 1059 W/m^2. Eight Calibrated thermocouples (K-type) are attached with upper surface of the absorber plate for measurement of plate average temperature, and two thermocouples is connected at entry section to find inlet temperature and two is used for measuring exit temperature of the air. A block diagram of the experimental set-up and Cross sectional view of Duct shown in fig.4.1(a) & 4.1(b)

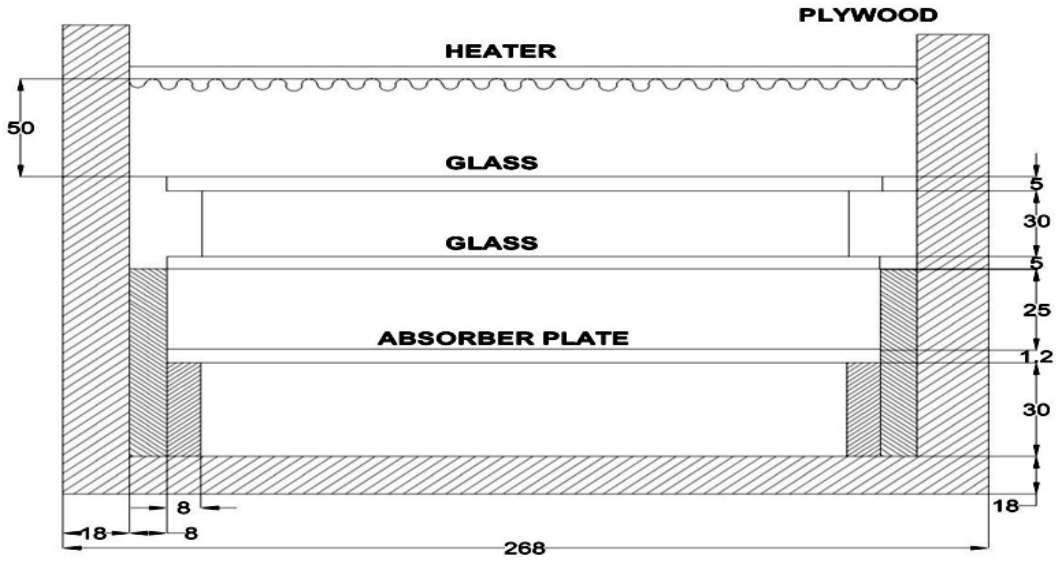

Fig.4.1(b)Cross sectional view of duct

Fig.4.2 (a) Experimental setup photograph

Fig.4.2 (b) Experimental setup photograph

4.2. Component of Experimental set up

(i) Air Heater Duct

The duct carries the roughness element on the absorber plate. The duct has provision to draw the ambient air with the help of blower. It has made of 1700mm × 400mm ×30mm wooden piece of 18 mm thickness with 12mm thermocoal insulation. For the turbulent flow regime, ASHRAE standard 93-77[14] recommends entry and exit length of 5√WH and 2.5√WH, respectively. The test section is of length 1500mm, the entry and exit length are 400mm and 200mm respectively.

(ii) Absorber Plates

Absorber plate is made of G.I. sheet (black painted 20 S.W.G.) of 1.2mm thick, 1500mm length and 220mm width were used in the solar air heater duct. The effective width of absorber plate is 200mm while 10mm on each side rested on the wooden supports. Artificial roughness of small diameter wires was used in the form multi- v shaped with gap. The wires were glued on the backside of the absorber plate with the help of flex. Gluing was carried out according to the

required pitch and angle of attack. It was ensured that these wires remain constant with the absorber plate as far as possible. Schematic diagram of roughness geometry and typical photograph of absorber plate is shown in Fig. 4.3(a) & 4.3(b)

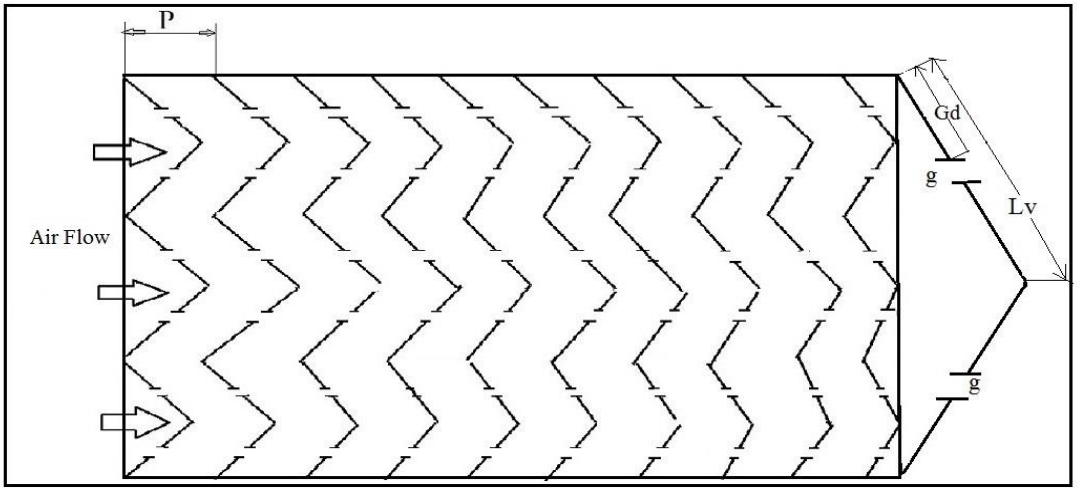

Fig.4.3 (a) Schematic diagram of roughness geometry

Fig.4.3 (b) Photograph of Smooth and Roughened Plate

(ii) **Electric Heater**

The electric heater plate is made up of asbestos sheet of 1500mm×400mm and 5mm thickness. The heating element is nichrome wire of 25 SWG (i.e. 0.0179 inches diameter). The heat is provided with constant heat flux of 1139W/m^2 to the absorber plate. A typical photograph of electric heater is shown in Fig. 4.4

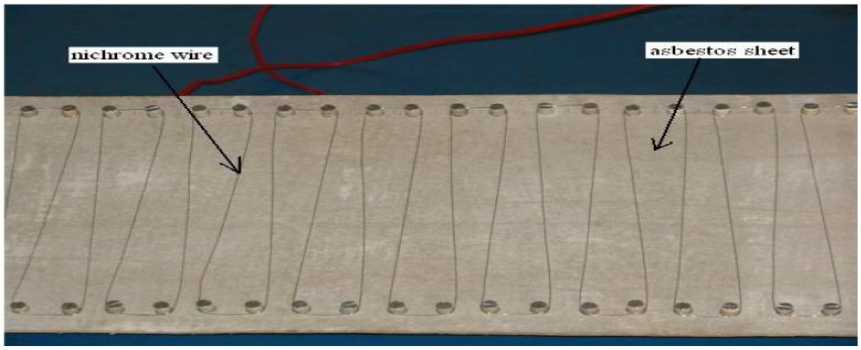

Fig.4.4 Electric Heater

(iv) **Blower**

The air is sucked through the rectangular duct by means of a blower. It is driven by a 3-phase 440V, 2.3kW and 1420rpm, A.C. motor. Air will sucked simultaneously through the duct at the desired mass flow rates. A gate valve is used for control of the air flow rate through the system. A typical photograph blower is shown in Fig. 4.5

Fig.4.5 High pressure Blower

(vi) **Insulation**

A 25mm cotton wool of thermal conductivity 0.029 W/m K was applied as insulation. The top side of entry and exit section of the duct is covered with smooth face of 12mm thick plywood.

4.3 Measurements

4.3.1 Measurement of Air Flow

It is accomplished by a flange type orifice meter fitted in the 50mm diameter pipe that carried the total air flow from the duct system. The mass flow rate through the orifice meter could be expressed in terms of the physical parameters of the orifice meter and the pressure difference across it, by an expression.

$$\mathbf{m} = \boldsymbol{C_d A_o} \sqrt{\frac{\boldsymbol{2\rho(\Delta P_O)}}{\boldsymbol{1-\beta^4}}} \qquad (4.1)$$

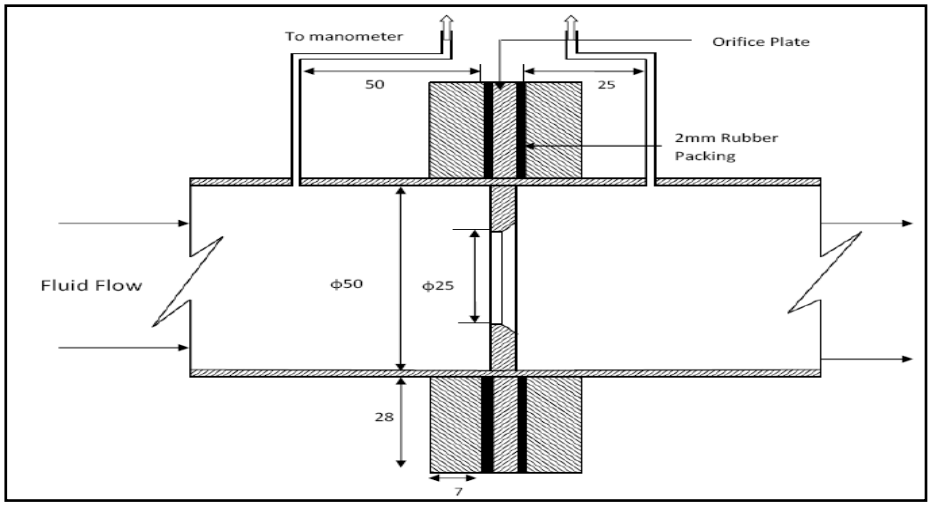

Fig.4.6 Orifice Meter (All Dimensions are in mm)

4.3.2 Temperature Measurement

Measurement of the temperature of absorber plate and duct air by using K-type copper aluminium thermocouples (28 SWG). Thermocouples are attached on the topside of the absorber plates at ten locations. The thermocouple locations are shown in Fig. 4.7 Temperature readings are note down by means of Digital temperature indicator shown in Fig. 4.8. Ambient air temperature is measured by using a standard mercury thermometer.

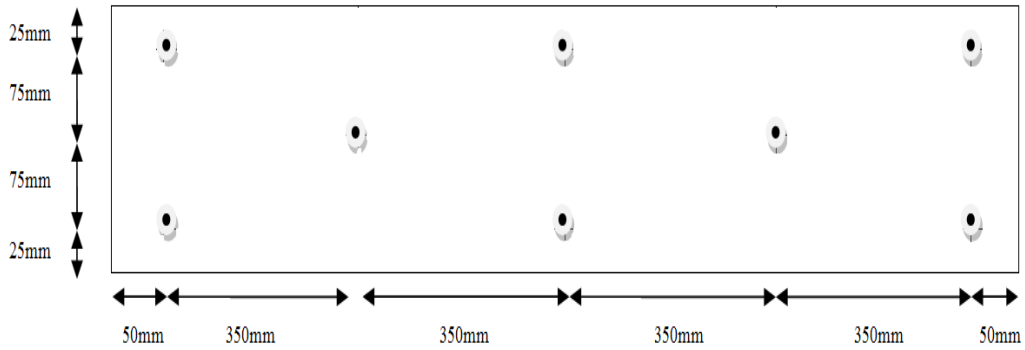

Fig.4.7 Position of Thermocouple (All dimensions in mm)

Fig.4.8 Thermocouple and temperature indicator cum selector switch

4.3.3 Pressure drop across the test section

In counter-flow air heater has a U-return section and extra duct length for air passage compared with conventional heaters. Hence, the extra pressure drop introduced by this design. The pressure drop in the U-section is the function of friction factor, which is measured by conventional micro manometer and Air flow meter.

$$\Delta P_d = \rho_w g \Delta h \sin\theta \tag{4.2}$$

$$f = \frac{2\Delta P_d D_h}{4\rho_d L V^2} \tag{4.3}$$

4.4 Experimental Data Reduction

The data includes thermocouple reading and air mass flow rates. This data have been deduced to obtain the average plate temperature, average air temperature, velocity of air flow in the duct, friction characteristics of the duct and the value of heat transfer coefficient. The data calculated by using formula.

(i) Average Temperature

The average flow temperature T_f is the measure value at the inlet and outlet of the test section by using the following equation,

$$T_f = \frac{(T_i + T_O)}{2} \tag{4.4}$$

Where,

T_i = inlet temperature (°C)

T_o = outlet temperature (°C)

(ii) Mass Flow Rate

Mass flow rate, m, has been determine from the pressure drop measurement across the orifice plate,

$$\mathrm{m} = cd\, A_0 \sqrt{\frac{2\rho(\Delta P_o)}{1-\beta^4}} \tag{4.5}$$

Calibration of orifice plate against a standard pitot tube, where $C_d = 0.624$ (coefficient of discharge) and $\Delta P_o = 9.81 \rho_m \Delta h_o \sin\theta$.

(iii) Heat Gain by the Air

Heat gain by the air calculated by the following equation,

$$\boldsymbol{Q_{air} = \dot{m} C_P (T_O - T_i)} \quad (4.6)$$

(iv) Heat Transfer Coefficient

The value of heat transfer coefficient between the absorber plate and fluid is given by the equation,

$$\dot{m} \boldsymbol{C_P [t_o - t_i] = h A_P [t_p - t_f]} \quad (4.7)$$

$$\boldsymbol{h = \frac{Q_{air}}{A_P (T_P - T_f)}}$$

Where,

Q_{air} = heat input to air (KJ) Cp = specific heat of air (KJ/kg-K)

T_p = temperature of plate (^{0}C) Tf = temperature of fluid (°C)

T_i = temperature at entry (^{0}C) To = temperature at exit (°C)

(v) Velocity Measurement

Velocity measurement by the following equation,

$$\boldsymbol{V = \frac{\dot{m}}{\rho \times w \times h}} \quad (4.8)$$

Where,

m = mass flow rate, kg/s w = width of the duct, m

h= height of the duct, m ρ = density of air, kg/m^3

(vi) Reynolds Number

The value of Reynolds number measurement by the following equation-

$$\boldsymbol{Re = \frac{\rho V D_h}{\mu}} \quad (4.9)$$

Where,

V= velocity of air (m/s) D_h = hydraulic diameter (m)

P = density of air (kg/m^3) μ = viscosity of air (m^2/s)

(vii) Friction factor

The friction factor is determined from the measured values of pressure drop, $(\Delta_p)_d$, across the test section length, L_f, of 1.5 m.

$$f = \frac{2(\Delta P)_d D_h}{4\rho L_f V^2} \quad (4.10)$$

$$(\Delta p)_d = (\Delta h)_d \times 9.81 \times \rho_m$$

Where, $(\Delta P)_d$ is pressure drop across the duct and $(\Delta h)_d$ MM reading, mm

(viii) Hydraulic Diameter

$$D_h = \frac{4WH}{2(W+H)} \quad (4.11)$$

(ix) Nusselt Number

$$N_u = \frac{hD_h}{k} \quad (4.12)$$

Where,

h= heat transfer coefficient (W/m^2K) D_h= hydraulic diameter (m)

K= thermal conductivity of air (W/ m K)

(x) Thermal Efficiency

$$\eta = \frac{GC_{P(T_0 - T_i)}}{I} \quad (4.13)$$

$$G = \frac{\dot{m}}{A_p}$$

Where,

G = mass velocity ($kg/s\text{-}m^2$) Ap = area of the plate (m^2)

I = heat flux (W/m**)**

Table No 4.1 - Experimental Data of Smooth Plate

Run No.	Head In cm of Water (Δh)	Thermocouple Reading											Pressure Drop In Duct In N/mm^2
		Inlet Air Temperature In °C	Absorber Plate Temperature In °C								Outlet Air Temperature In °C		
		T_i	T_1	T_2	T_3	T_4	T_5	T_6	T_7	T_8	To_1	To_2	ΔP_d
1	1	37	86	87	90	91	89	90	86	84	48	48	1.49
2	4	36	79	80	84	86	85	84	82	81	47	43	2.89
3	8	36	76	77	81	83	82	80	77	75	42	42	4.11
4	14	35	75	76	80	82	80	79	75	74	40	39	5.75
5	22	35	65	69	76	80	87	83	77	75	39	39	6.78
6	32	36	62	65	70	77	74	69	62	61	40	39	8.22
7	42	35	57	59	66	70	69	64	56	53	39	38	10.78

Table No 4.2 - Experimental Data of Roughened Duct (plate-1)

Roughness Data: (p/e) = 10, (e/D) = 0.043, $\alpha = 60^0$ G_d/L_v=0.42

Run No.	Head In cm of Water (Δh)	Thermocouple Reading											Pressure Drop In Duct In N/mm^2
		Inlet Air Tempera-ture In °C	Absorber Plate Temperature In °C								Outlet Air Temperature In °C		
		T_i	T_1	T_2	T_3	T_4	T_5	T_6	T_7	T_8	To_1	To_2	ΔP_d
8	1	39	82	84	91	93	90	90	87	86	57	55	2.40
9	4	39	79	81	85	87	86	84	82	79	55	53	5.04
10	8	39	73	76	79	80	78	74	73	70	52	51	6.68
11	14	38	62	66	72	74	72	70	69	66	50	50	9.25
12	22	38	56	60	63	66	68	63	62	61	48	47	10.58
13	32	38	48	50	53	66	65	63	60	55	46	45	13.86
14	42	37	46	47	50	58	60	58	56	54	45	45	15.80

Table No 4.3 - Experimental Data of Roughened Duct (plate-2)

Roughness Data: (p/e) = 10, (e/D) = 0.043, $\alpha = 60^0$ G_d/L_v=0.55

Run No.	Head In cm of Water (Δh)	Thermocouple Reading											Pressure Drop In Duct In N/mm^2
		Inlet Air Temperature In °C	Absorber Plate Temperature In °C								Outlet Air Temperature In °C		
		T_i	T_1	T_2	T_3	T_4	T_5	T_6	T_7	T_8	To_1	To_2	ΔP_d
15	1	39	78	81	83	84	82	80	78	77	58	57	2.67
16	4	39	73	75	79	79	80	76	72	71	55	53	5.09
17	8	38	66	71	76	77	76	72	67	65	53	49	7.49
18	14	38	63	65	67	68	67	66	62	60	49	49	9.80
19	22	38	58	61	63	66	65	63	61	60	48	47	12.42
20	32	38	54	58	62	63	61	57	56	54	47	45	15.12
21	42	37	48	53	57	61	57	56	54	53	45	45	16.90

Table No 4.4 - Experimental Data of Roughened Duct (plate-3)

Roughness Data: (p/e) = 10, (e/D) = 0.043, $\alpha = 60^0$ G_d/L_v=0.69

Run No.	Head In cm of Water (Δh)	Thermocouple Reading											Pressure drop in Duct in N/mm^2
		Inlet air Tempera-ture in °C	Absorber Plate Temperature In °C								Outlet air Temperature in °C		
		T_i	T_1	T_2	T_3	T_4	T_5	T_6	T_7	T_8	To_1	To_2	ΔP_d
22	1	39	73	74	78	78	79	77	74	74	63	63	3.58
23	4	37	69	71	72	75	74	73	72	69	58	56	6.86
24	8	37	60	61	64	67	66	65	63	60	54	43	9.92
25	14	36	56	59	60	60	58	56	55	54	50	49	13.87
26	22	36	52	53	55	57	56	53	52	49	48	47	16.53
27	32	36	51	54	54	56	54	52	49	46	47	47	20.02
28	42	36	49	51	52	54	53	52	46	46	46	46	22.96

Table No 4.5 - Experimental Data of Roughened Duct (plate-4)

Roughness Data: (p/e) = 10, (e/D) = 0.043, $\alpha = 60^0$ G_d/L_v=0.80

Run No.	Head In cm of Water (Δh)	Thermocouple Reading											Pressure Drop In Duct In N/mm^2
		Inlet Air Tempera-ture In °C	Absorber Plate Temperature In °C								Outlet Air Temperature In °C		
		T_i	T_1	T_2	T_3	T_4	T_5	T_6	T_7	T_8	To_1	To_2	ΔP_d
29	1	37	85	86	87	88	87	85	83	81	50	50	4.93
30	4	36	75	77	81	83	82	81	77	76	47	48	9.56
31	8	36	69	70	73	75	74	72	71	68	44	44	13.84
32	14	36	65	66	69	71	70	69	67	66	44	43	19.05
33	22	35	60	61	65	67	66	64	61	59	42	41	23.16
34	32	35	54	57	59	60	62	58	54	51	41	40	25.64
35	42	35	52	53	57	58	55	55	51	50	40	40	26.97

CHAPTER–5

RESULTS AND DISCUSSION

This chapter summarizes the result of heat transfer obtained from experiment as mention in chapter-4 for varying relative gap distance and Reynolds number. The value of Nusselt number for the four sided smooth duct have also been determined to facilitate the comparison of roughened duct data with smooth data.

The experimental investigation encompassed the Reynolds number (Re) range from 2000 to 15,000, relative width ratio (W/w) of 3, relative gap distance (G_d/L_v) of 0.42-0.80, relative gap width (g/e) of 0.5-1.5, relative roughness height (e/D) of 0.043, relative roughness pitch (P/e) of 10, angle of attack (α) of 60°.

5.1 Validation of Experimental Data

To validate the results of present work for heat transfer in the form of Nusselt number determined from experimental data are compared with the analytical values obtained from Dittus-Boelter equation.The Nusselt number for a smooth rectangular duct is given by the Dittus-Boelter equation is –

$$Nu_s = 0.023Re^{0.8}Pr^{0.4} \quad (5.1)$$

The comparison of experimental and predicted values from equation of Nusselt number has been shown in Graph 5.1

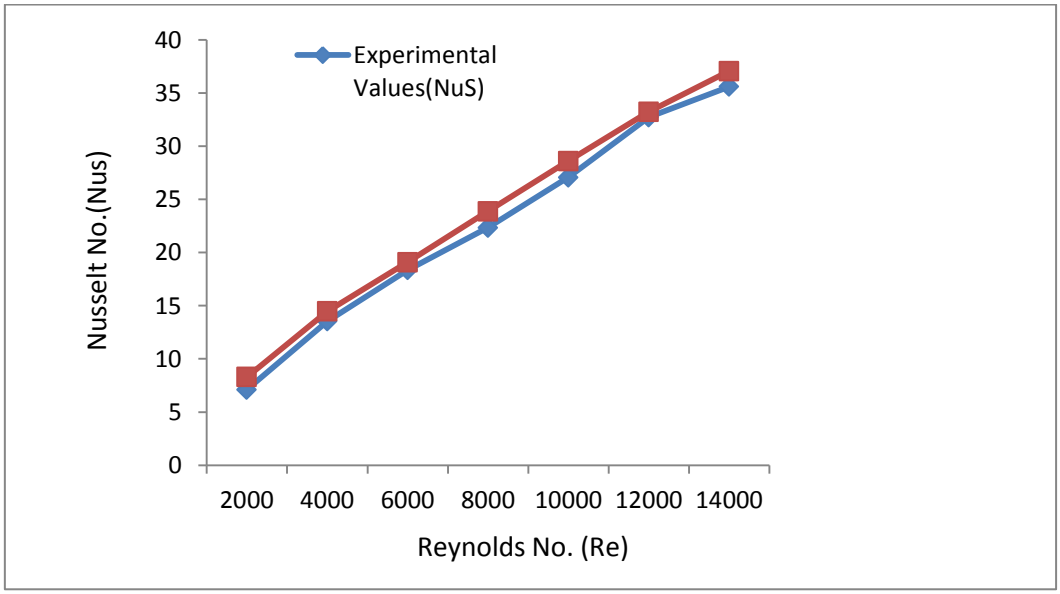

Graph 5.1 Comparison of experimental and predicted values of Nusselt number of smooth surface

5.2 Effect of Relative gap Distance on Nusselt number

Graph 5.2 shows that the effect of different relative gap distance on the Nusselt number for the multi v-shape ribs with gap having a fixed relative gap width (g/e) 1.0. It shows the Nusselt number increase with increase in relative gap distance and attains the maximum at a relative gap distance of 0.69 and thereafter it decreases with increases in relative gap distance. For any fixed value of Reynolds number the value of Nusselt number increases with increasing in the value of relative roughness height because of the increase in turbulence. The numerical values of Nusselt number obtained by experimental are given in table 5.1.

Table 5.1 Nusselt number of smooth and roughened plate

Run No.	Head (cm)	Reynolds number	Nusselt Number				
			smooth	Gd/Lv=0.42	Gd/Lv=0.55	Gd/Lv=0.69	Gd/Lv=0.80
1	1	1909.9	7.12	12.36	16.91	24.83	9.14
2	4	3819.9	11.54	24.22	30.24	37.22	17.13
3	8	5402.2	14.56	32.66	40.59	50.21	21.21
4	14	7146.4	18.4	48.52	57.42	68.2	29.58
5	22	8958.5	22.07	66.15	78.13	88.51	36.69
6	32	10804.4	28.73	79.86	91.21	105.7	48.23
7	42	12378.1	36.3	95.5	110.63	125.04	58.58

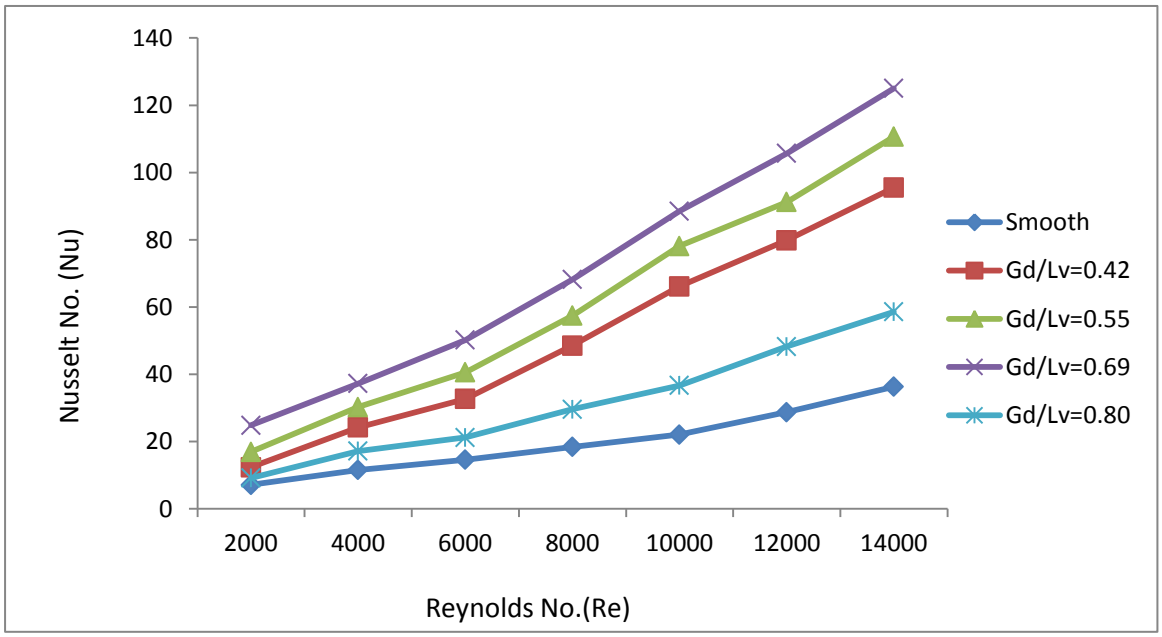

Graph 5.2 Effect of relative gap distance on Nusselt number

5.3 Variation of Thermal Efficiency with Reynolds number for Relative gap Distance

Graph 5.3 shows the variation of Thermal Efficiency with Reynolds number for different relative gap distance. For a fixed value of relative gap distance (Gd/Lv=0.42) the efficiency increases with the Reynolds number. The maximum efficiency is found at a relative gap distance on 0.69 with a relative gap width 1.0 and relative roughness pitch 10.

Table 5.2 Thermal Efficiency of smooth and roughened plate

Run No.	Head (cm)	Reynolds number	Thermal Efficiency				
			smooth	Gd/Lv=0.42	Gd/Lv=0.55	Gd/Lv=0.69	Gd/Lv=0.80
1	1	1909.9	13.54	22.01	26.13	29.9	18.36
2	4	3819.9	21.43	34.38	37.38	42.51	28.49
3	8	5402.2	28.43	45.23	49.24	53.21	36.15
4	14	7146.4	32.01	52.04	56.71	61.34	41.23
5	22	8958.5	36.74	56.53	61.53	68.9	45.65
6	32	10804.4	39.24	60.51	65.55	74.34	49.37
7	42	12378.1	43.03	65.48	69.84	78.45	53.15

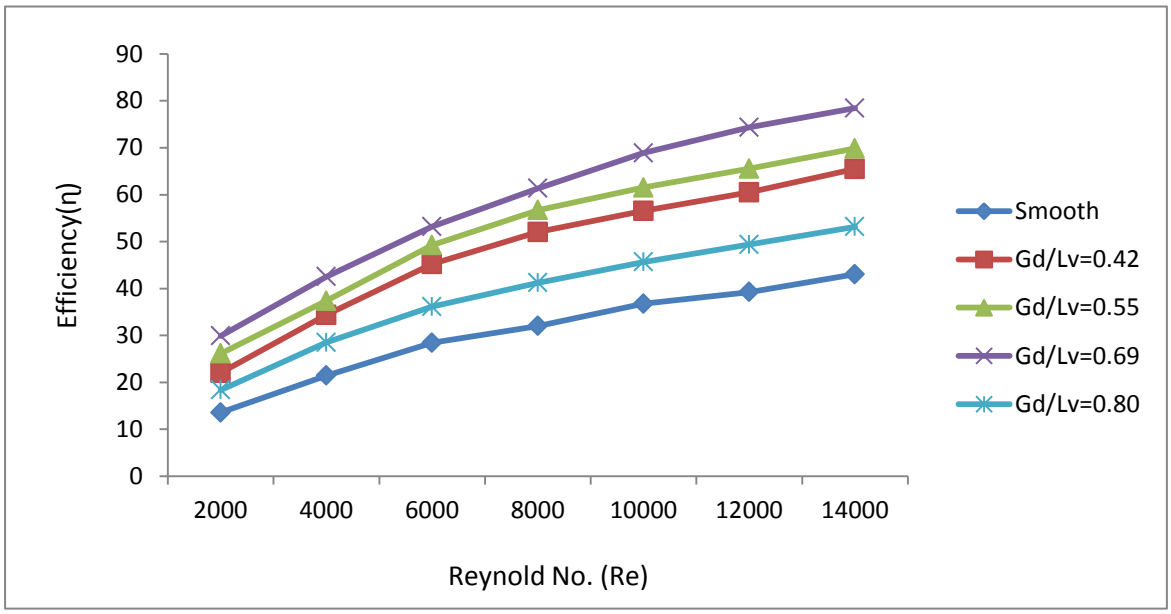

Graph 5.3 Variation of Thermal Efficiency with Reynolds number for relative gap distance

As the value of Reynolds number increases turbulence in the air flow increases thus more heat transfer takes place from absorber plate to air, due to increases in

turbulence at higher Reynolds number thus the thermal efficiency increases while at lower Reynolds number the efficiency is very low due to the presence of laminar sub layer which offer resistance to heat transfer from absorber plate to flowing air and hence lower thermal efficiency is observed. Table 5.2 shows the thermal efficiency of smooth and roughed plate.

5.4 Effect of Relative gap Distance on Nusselt number ratio

Graph 5.4 shows that the effect of relative gap distance on Nusselt number ratio (Nu/ Nu_s) for smooth plate with roughed plate of the multi v-shape ribs with gap having a fixed relative gap width (g/e) 1.0. The Nusselt number ratio increase with increase in Reynolds number. The value of Nusselt number ratio is less for relative gap distance of 0.80 and the maximum at relative gap distance of 0.69. Table 5.3 shows the Nusselt number ratio.

Table 5.3 Nusselt number ratio

Run No.	Head (cm)	Reynolds number	Nusselt Number Ratio			
			Gd/Lv=0.42	Gd/Lv=0.55	Gd/Lv=0.69	Gd/Lv=0.80
1	1	1909.9	1.63	1.98	2.37	1.39
2	4	3819.9	1.95	2.32	2.76	1.66
3	8	5402.2	2.19	2.63	3.1	1.87
4	14	7146.4	2.42	2.89	3.46	2.06
5	22	8958.5	2.61	3.14	3.71	2.19
6	32	10804.4	2.77	3.28	3.89	2.31
7	42	12378.1	2.82	3.36	4	2.38

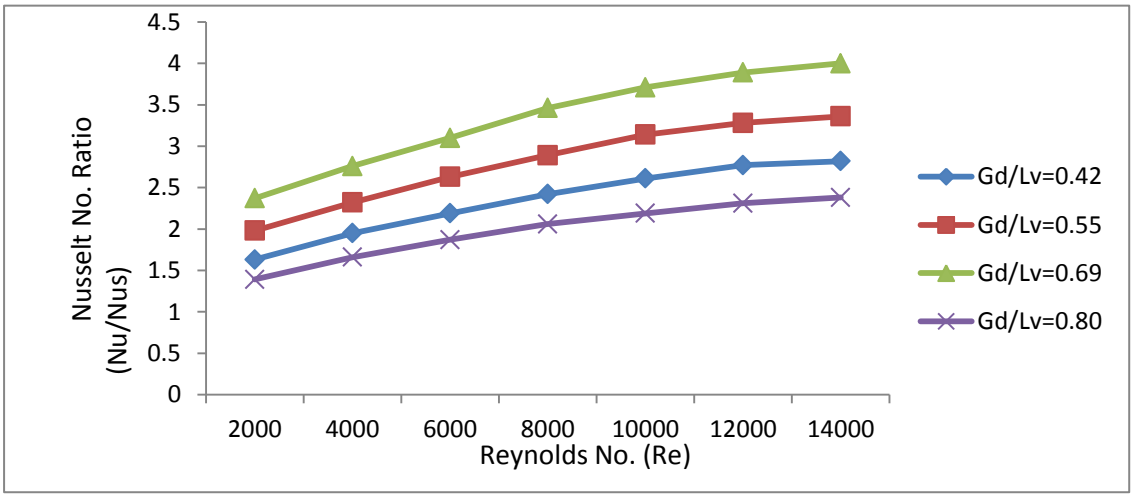

Graph 5.4 Effect of relative gap distance on Nusselt number ratio

5.5 Effect of Relative gap Distance on Heat transfer Coefficient

Graph 5.5 shows that the effect different relative gap distance on the heat transfer coefficient for the multi v-shape ribs with gap having a fixed relative gap width (g/e) 1.0. It can be seen that the heat transfer coefficient increases with increase in Reynolds number for all cases due to increase in turbulence as the value of Reynolds number increases. For a fixed value of relative gap distance (Gd/Lv=0.42) the heat transfer coefficient increases with the Reynolds number. The heat transfer coefficient is maximum for the rough plate at a relative gap distance of 0.69. The numerical values of heat transfer coefficient obtained by experimental are given in table 5.4.

Table 5.4 Heat Transfer Coefficient of smooth and roughened plate

Run No.	Head (cm)	Reynolds number	Heat Transfer Coefficient				
			smooth	Gd/Lv=0.42	Gd/Lv=0.55	Gd/Lv=0.69	Gd/Lv=0.80
1	1	1909.9	3.65	6.34	8.68	11.54	5.69
2	4	3819.9	4.54	12.43	15.52	18.24	7.3
3	8	5402.2	5.45	17.79	20.83	24.05	10.8
4	14	7146.4	7.36	21.47	26.48	32.08	15.18
5	22	8958.5	9.22	28.9	33.98	40.26	18.83
6	32	10804.4	13.12	34.4	40.71	49.58	24.75
7	42	12378.1	18.22	42.4	49.78	60.26	30

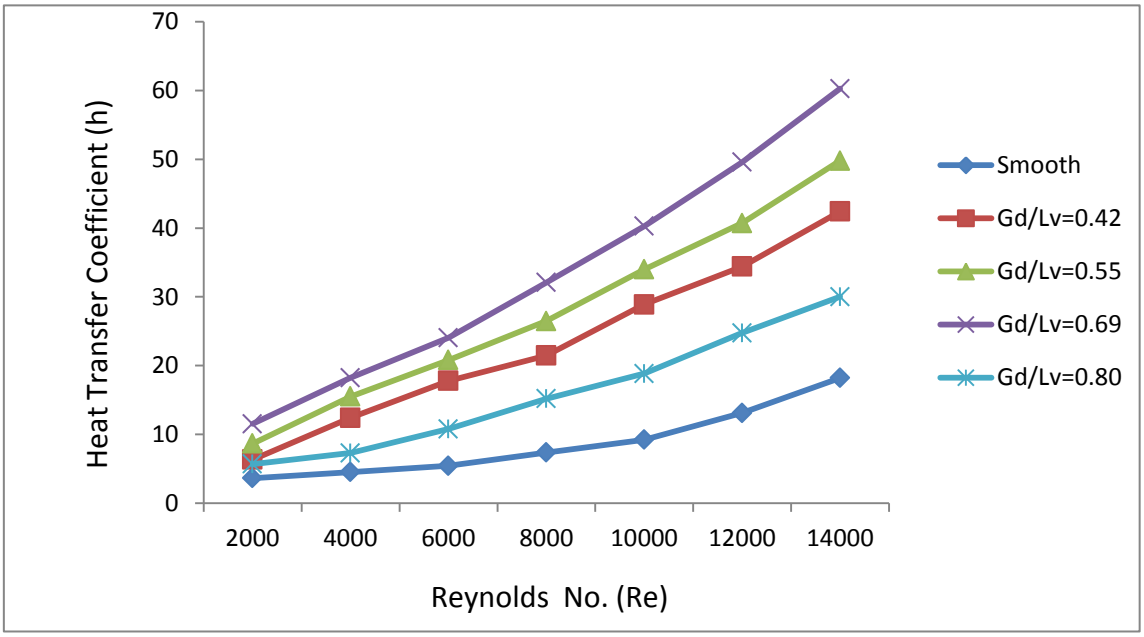

Graph 5.5 Effect of relative gap distance on Heat transfer coefficient

CHAPTER–6

CONCLUSION AND FUTURE SCOPE

6.1 Conclusion

The following conclusion can be drawn from the experimental work-

1. Introduction of artificial roughness on under side of the absorber plate enhances Nusselt Number and Heat transfer coefficient compare to smooth duct.
2. Providing gap in multi v-shaped rib result in increasing in heat transfer coefficient of air flow duct.
3. It has been found that the artificial roughness applied on heat transferring surface breaks the viscous sub-layer to reduce thermal resistance close to the surface.
4. The maximum value of Nusselt number and friction factor are observed in multi v-shaped with a relative gap distance of 0.69 and relative gap width of 1.0.
5. Thermal efficiency roughed plates has been compared with the smooth duct and the maximum the efficiency shows in roughed plate at a relative gap distance of 0.69 and relative gap width of 1.0.

6.2 Future Scope

In the present work, an attempt has been made to study the enhancement of solar collector performance using artificial roughness. Only one particular roughness configuration i.e. circular in shape was considered on the bottom surface of the absorber plate in the collector duct. The collector was modeled as a rectangular duct.

Since the selection of a roughness geometry that results in optimum heat transfer performance depends upon a very careful matching of roughness parameters and flow parameters, an elaborate experimental study involving different roughness configurations such as semicircular cross section, square and triangular at different relative roughness height (e/D_h) and relative roughness pitch (p/e) ratios can be made to arrive at an optimum set of roughness parameters.

The present study involves air as the carrier fluid. However the present work can be extended for different fluids.

REFERENCES

[1] Gupta D, Solanki SC, Saini JS. Thermo hydraulic performance of solar air heaters with roughened absorber plates. Solar Energy 1997; 61:33-42.

[2] Varun, Saini RP, Singal SK. Investigation of thermal performance of solar air heater having roughness elements as a combination of inclined and transverse ribs on the absorber plate. Renewable Energy 2008; 33:1398–405.

[3] Prasad BN, Saini JS. Effect of artificial roughness on heat transfer and friction factor in a solar air heater. Solar Energy 1988; 41(6):555–60.

[4] Sahu MM, Bhagoria JL. Augmentation of heat transfer coefficient by using 90° broken transverse ribs on absorber plate of solar air heater. Renewable Energy 2005; 30:2057–63.

[5] Momin AME, Saini JS, Solanki SC. Heat transfer and friction in solar air heater duct with V-shaped rib roughness on absorber plate. International Journal of Heat and Mass Transfer 2002; 45:3383–96.

[6] Singh S, Chander S, Saini JS. Heat transfer and friction factor correlations of solar air heater ducts artificially roughened with discrete V-down ribs. Energy 2011; 36:5053-64.

[7] Lanjewar A, Bhagoria JL, Sarviya RM. Heat and friction in solar air heater duct with W-shaped rib roughness on absorber plate. Energy2011; 36: 4531-4541.

[8] Kumar A, Bhagoria JL, Sarviya RM. Heat transfer enhancement in channel of solar air collector by using discrete W-shaped artificial roughened absorber International 19th national & 8th ISHMTASME heat and mass transfer conference 2008.

[9] Jaurker AR, Saini JS, Gandhi BK. Heat transfer and friction in solar air heater duct with rib and groove shaped rib roughness on absorber plate. Solar energy 2006; 80(8):895–907.

[10] Saini RP, Saini JS. Heat transfer and friction factor correlations for artificially roughened ducts with expended metal mesh as roughness element. International Journal of Heat and Mass Transfer 1997; 40(4):973–86.

[11] Sopian K, Alghoul MA, Alfegi Ebrahim M, Sulaiman MY, Musa EA. Evaluation of thermal efficiency of double-pass solar collector with porous-nonporous media. Renewable Energy 2009; 34:640-645.

[12] Sopian K, Supranto WRW, Daud MY, Othman BY. Thermal performance of the double-pass solar collector with and without porous media. Renewable Energy 1999; 18:557-564

[13] Prasad SB, Saini JS, Singh KM. Investigation of heat transfer and friction characteristics of packed bed solar air heater using wire mesh as packing material. Solar Energy 2009; 83:773-783.

[14] Bhagoria JL, Saini JS, Solanki SC. Heat transfer coefficient and friction factor correlations for rectangular solar air heater duct having transverse wedge shaped rib roughness on the absorber plate. Renew Energy 2002; 25:341–369.

[15] ASHRAE standard 93–77. Method of testing to determine the thermal performance of solar collector, 1977.

[16] S. P. Shukhatme, a Text book of solar energy, Tata, McGraw-Hill publication (1996).

[17] Ho CD, Yeh HM, Wang RC. Heat-transfer enhancement in double-pass flat plate solar air heaters with recycles. Energy 2005; 30:2796-2817.

[18] Esen H. Experimental energy and exergy analysis of a double-flow solar air heater having different obstacles on absorber plates. Building and Environment 2008; 43:1046-1054.

[19] Lertsatitthanakorn C, Khasee N, Atthajariyakul S, Soponronnarit S,Therdyothin A, Suzuki RO. Performance analysis of a double-pass thermoelectric solar air collector. Solar Energy Materials & Solar Cells 2008; 92:1105-1109.

[20] Ozgen F, Esen M, Esen H. Experimental investigation of thermal performance of a double-flow solar air heater having aluminium cans. Renewable Energy2009; 34:2391-2408.

[21] Aharwal KR, Gandhi BK, Saini JS. Experimental investigation on heat-transfer enhancement due to a gap in an inclined continuous rib arrangement in a rectangular duct of solar air heater. Renewable Energy 2008; 33:585–96.

[22] Saini JS. Heat transfer and friction factor correlations of solar air heater ducts artificially roughened with discrete V-down ribs. Energy 2011 36:5053-5064.